

**University of Alberta**

**Deciphering the Claudins that Mediate Renal Calcium Reabsorption**

by

**Prajakta Vivek Desai**

A thesis submitted to the Faculty of Graduate Studies and Research  
in partial fulfillment of the requirements for the degree of

**Master of Science**

**Medical Sciences-Pediatrics**

©Prajakta Vivek Desai

Fall 2012

Edmonton, Alberta

Permission is hereby granted to the University of Alberta Libraries to reproduce single copies of this thesis and to lend or sell such copies for private, scholarly or scientific research purposes only. Where the thesis is converted to, or otherwise made available in digital form, the University of Alberta will advise potential users of the thesis of these terms.

The author reserves all other publication and other rights in association with the copyright in the thesis and, except as herein before provided, neither the thesis nor any substantial portion thereof may be printed or otherwise reproduced in any material form whatsoever without the author's prior written permission.

## ABSTRACT

Kidney stones and osteoporosis are prevalent clinical conditions posing a large economic burden to the healthcare system. A common risk factor for both these diseases is hypercalciuria, which is the inappropriate excretion of calcium in urine. Changes in serum calcium levels are detected by the calcium sensing receptor (CaSR). In the kidney, the CaSR is localized in tubular segments where calcium ( $\text{Ca}^{2+}$ ) flux occurs via the paracellular pathway, specifically the proximal tubule and the thick ascending limb of Henle's loop (TAL). Claudins are proteins localized in the tight junction of epithelia that control paracellular ion flux. Recently, claudin-14 (Cldn14) expression was observed in the TAL. We found that Cldn14 is regulated by dietary  $\text{Ca}^{2+}$  intake and by elevated serum  $\text{Ca}^{2+}$  levels after prolonged 1,25-dihydroxyvitamin  $\text{D}_3$  administration in mice. Consistent with this, *in vivo* activation of the CaSR by administration of the calcimimetic Cinacalcet, lead to a 40-fold increase in Cldn14 mRNA abundance. Overexpression of Cldn14 in a renal tubular cell culture model inhibited paracellular  $\text{Ca}^{2+}$  flux. Together the data suggests that when serum  $\text{Ca}^{2+}$  level increases it activates the CaSR leading to increased Cldn14 expression in the TAL. This in turn blocks  $\text{Ca}^{2+}$  reabsorption and induces calciuria. Dysregulation of this newly described CaSR-Cldn14 axis likely contributes to the development of hypercalciuria and kidney stones.

## ACKNOWLEDGEMENTS

It is a pleasure to thank my supervisor Dr. Todd Alexander for giving me the opportunity to come to Canada and be a part of this wonderful project. His patience, encouragement and enthusiasm towards science have been the basis of this project. His way of approaching challenges and immense knowledge has made the past 2 years a lot easier. He is one of the best teachers and supervisors I have had.

A special thanks to Dr. Henrik Dimke whose ideas for this project are of great value and this thesis would not have been possible without his contribution. I would like to thank all the members of the Alexander lab who made the working environment bright and light. I am thankful to Wanling Pan for teaching and guiding me in all the techniques. It was a pleasure working with Alyssa Lau, Jelena Borovac and Juraj Rievaj. I would like to thank Devishree Krishnan for being a great colleague in the lab and a dear friend outside the lab.

I would also like to thank my committee members Dr. Branko Braam and Dr. Po-Yin Cheung for their guidance. I am thankful to Dr. Emmanuelle Cordat and Dr. Joe Casey for all their valuable advice. I acknowledge Alberta Heritage Foundation for Medical Research and the Kidney Foundation of Canada for their financial support. I appreciate the scientific discussions I have had with all my friends that has helped me understand science in a simple way. I am grateful to all my friends in Canada who have made life away from work all happy and cherishable.

I am deeply grateful to my parents Vivek and Meenakshi Desai for believing and supporting me throughout. My sister Radhika and brother-in-law Salil have been a constant source of motivation; I thank them for all the faith they showed in me. To my family I dedicate my thesis.

## TABLE OF CONTENTS

<b>Chapter 1: Introduction</b> .....	1
<b>1.1 Kidney stones</b> .....	2
1.1.1 Prevalence.....	2
1.1.2 Pathogenesis.....	2
1.1.3 Types and causes of kidney stones.....	4
1.1.4 Associated diseases.....	5
1.1.5 Treatment.....	5
<b>1.2 Osteoporosis</b> .....	6
1.2.1 Prevalence.....	6
1.2.2 Pathophysiology.....	6
1.2.3 Treatment.....	7
<b>1.3 Calcium homeostasis</b> .....	8
<b>1.4 Calcium flux across the nephron</b> .....	10
1.4.1 Glomerular filtration.....	10
1.4.2 Paracellular vs transcellular transepithelial reabsorption.....	10
1.4.3 Calcium flux across the proximal tubule.....	13
1.4.4 Calcium flux across the thick ascending limb.....	13
1.4.5 Calcium flux across the distal nephron.....	14
<b>1.5 Claudins</b> .....	15
1.5.1 Structure and function.....	15
1.5.2 Expression, function and mutations in claudins.....	16
1.5.2.1 Claudin 2.....	16
1.5.2.2 Claudin 10.....	17
1.5.2.3 Claudin 12.....	17
1.5.2.4 Claudin 14.....	17
1.5.2.5 Claudin 16.....	18
1.5.2.6 Claudin 19.....	18
<b>1.6 Hypercalciuria</b> .....	19
<b>1.7 Thesis Hypothesis</b> .....	22
<b>1.8 Thesis Objectives</b> .....	22

<b>Chapter 2: Materials and Methods</b> .....	23
<b>2.1 Animals</b> .....	24
<b>2.2 Isolation of whole kidney and proximal tubule RNA</b> .....	24
<b>2.3 Genomic DNA isolation</b> .....	24
<b>2.4 Complimentary DNA synthesis</b> .....	25
<b>2.5 Negative control for cDNA synthesis (noRT)</b> .....	25
<b>2.6 Determination of Gene Expression by Polymerase chain reaction (PCR)</b> .....	26
2.6.1 Expression primers.....	26
<b>2.7 Gel electrophoresis</b> .....	30
<b>2.8 Animal Experiments</b> .....	31
2.8.1 Experimental protocol 1 – altered calcium diets.....	31
2.8.2 Experimental protocol 2 - vitamin D <sub>3</sub> administration.....	31
2.8.3 Experimental protocol 3 – cinacalcet treatment.....	32
<b>2.9 Determination of solutes, creatinine and hormones</b> .....	33
2.9.1 Urinary calcium.....	33
2.9.2 Urinary creatinine.....	33
2.9.3 Plasma PTH assay.....	33
2.9.4 1,25- Dihydroxy Vitamin D Assay.....	34
<b>2.10 Real-time PCR</b> .....	35
2.10.1 RNA isolation.....	35
2.10.2 Quantitative PCR.....	35
<b>2.11 Immunostaining</b> .....	38
2.11.1 Antibodies and fluorescent stains.....	38
2.11.2 Validation of antibodies.....	39
<b>2.12 Statistical analysis</b> .....	40
<b>Chapter 3: Results</b> .....	41
<b>3.1 Expression of claudins in kidney</b> .....	42
<b>3.2 Ca<sup>2+</sup> diet experiment</b> .....	46
3.2.1 Blood and Urinary data.....	46
3.2.2 RNA expression of claudins in whole kidney.....	53

<b>3.3 Vitamin D experiment</b> .....	56
3.3.1 Blood and urinary data.....	56
3.3.2 RNA expression of claudins in whole kidney.....	60
3.3.3 Cldn14 protein expression.....	60
<b>3.4 Cinacalcet experiment</b> .....	63
3.4.1 Blood and urinary data.....	63
3.4.2 RNA expression of claudins in whole kidney.....	66
3.4.3 Cldn14 protein expression.....	66
<b>3.5 Localization of Cldn14 in murine kidney</b> .....	69
<b>Chapter 4: Discussion</b> .....	72
<b>4.1 Renal claudin expression</b> .....	74
<b>4.2 Renal Cldn14 expression</b> .....	74
<b>4.3 Driving forces for calcium flux across the TAL</b> .....	76
<b>4.4 Cldn14, a blocker of the Cldn 16/19 pore?</b> .....	77
<b>4.5 Role of Cldn14 in human physiology and pathophysiology</b> .....	78
<b>Summary</b> .....	80
<b>Conclusion</b> .....	82
<b>Potential future directions</b> .....	83
<b>Bibliography</b> .....	84
<b>Appendix</b> .....	89

## LIST OF TABLES

Table 2.1. Primers to detect expression by PCR.....	28
Table 2.2. Real-time PCR primers and probes.....	37
Table 3.1A Calcium diet experiment (10 days): <i>Metabolic cage data</i> .....	47
Table 3.1B Calcium diet experiment (21 days): <i>Metabolic cage data</i> .....	47
Table 3.2A Calcium diet experiment (10 days): <i>Blood-gas analysis</i> .....	49
Table 3.2B Calcium diet experiment (21 days): <i>Blood-gas analysis</i> .....	49
Table 3.3A Calcium diet experiment (10 days): <i>Serum electrolytes</i> .....	50
Table 3.3B Calcium diet experiment (21 days): <i>Serum electrolytes</i> .....	50
Table 3.4A Calcium diet experiment (10 days): <i>Urine electrolytes</i> .....	51
Table 3.4B Calcium diet experiment (21 days): <i>Urine electrolytes</i> .....	51
Table 3.5A Calcium diet experiment (10 days): <i>Urine analysis</i> .....	52
Table 3.5B Calcium diet experiment (21 days): <i>Urine analysis</i> .....	52
Table 3.6 Calcium diet experiment (10 & 21 days): <i>RNA expression of 1<math>\alpha</math>-OHase and 24-OHase</i> .....	55
Table 3.7 Vitamin D experiment: <i>Metabolic cage data</i> .....	57
Table 3.8 Vitamin D experiment: <i>Blood-gas analysis</i> .....	57
Table 3.9 Vitamin D experiment: <i>Serum electrolytes</i> .....	59
Table 3.10 Vitamin D experiment: <i>Urine analysis</i> .....	59
Table 3.11 Vitamin D experiment: <i>Urine electrolytes</i> .....	59
Table 3.12 Vitamin D experiment: <i>RNA expression of 1<math>\alpha</math>-OHase and 24-OHase</i> .....	62
Table 3.13 Cinacalcet experiment: <i>Metabolic cage data</i> .....	64
Table 3.14 Cinacalcet experiment: <i>Blood-gas analysis</i> .....	64
Table 3.15 Cinacalcet experiment: <i>Serum electrolytes</i> .....	64
Table 3.16 Cinacalcet experiment: <i>Urine analysis</i> .....	64
Table 3.17 Cinacalcet experiment: <i>RNA expression of 1<math>\alpha</math>-OHase and 24-OHase</i> .....	68

## LIST OF FIGURES

Figure 1.1 Schematic representation of paracellular and transcellular transepithelial reabsorption along the nephron.....	12
Figure 3.1 Claudin expression in whole kidney.....	44
Figure 3.2. Claudin expression in microdissected proximal tubules.....	45
Figure 3.3: Calcium diet experiment (10 and 21 days)- <i>Blood and urine data</i> .....	48
Figure 3.4: Calcium diet experiment (10 and 21 days): <i>RNA expression of claudins in whole kidney</i> .....	54
Figure 3.5: Calcium diet experiment (10 days): <i>RNA expression of claudins in whole kidney</i> .....	55
Figure 3.6 Vitamin D experiment: <i>Blood and urine data</i> .....	58
Figure 3.7 Vitamin D experiment: <i>RNA expression of claudins in whole kidney</i> .....	61
Figure 3.8 Vitamin D experiment: <i>Immunostaining for Cldn14</i> .....	62
Figure 3.9 Cinacalcet experiment: <i>Blood and urine data</i> .....	65
Figure 3.10 Cinacalcet experiment: <i>RNA expression of claudins in whole kidney</i> .....	67
Figure 3.11 Cinacalcet experiment: <i>Immunostaining for Cldn14</i> .....	68
Figure 3.12 Immunostaining for claudin 14 in the proximal tubule.....	70
Figure 3.13 Immunostaining for claudin 14 in the TAL.....	71
Figure 4.1 Schematic representation of the proposed mechanism of CaSR activation and function of Cldn14 in the TAL.....	

**CHAPTER 1**  
**INTRODUCTION**

## **1.1 KIDNEY STONES**

### **1.1.1 Prevalence**

In the United States of America kidney stones occur in approximately 5% of women and 12% of men. The approximate cost of treatment to the American government is 2.1 billion annually (Evan AP 2010). This data is not available for Canada. A 4-fold rise in the number of children being diagnosed with kidney stones, from 1994-1996 to 2003-2005 has also been reported (Schissel and Johnson 2011). Predictions suggest that rising temperatures and salt consumption worldwide will contribute to an increase in the occurrence of kidney stones in both adults and children to an estimated 1.6-2.2 million lifetime cases by 2050 (Evan AP 2010).

### **1.1.2 Pathogenesis**

The pathogenesis of kidney stone formation is variable. As such no single mechanism can describe the formation of the various types of kidney stones. So far three major pathways have been identified that can lead to kidney stone formation.

The first pathway is overgrowth of interstitial apatite plaque. In this pathway, first a plaque is formed consisting of calcium phosphate (CaP). This usually occurs in the basement membrane of thin limbs of Henle's loop (Fedric L, Andrew P et al. 2010). A stone then starts to form on this plaque and continues growing for years. It is noteworthy that although a stone formed in this way may be composed of calcium oxalate, the initial plaque is always of calcium phosphate. It has been observed that

stones that get detached from their plaques have patches of phosphate on their concave surface and remain floating in the supersaturated fluid in that nephron segment. Further, the urothelial cell covering is lost at the sites of plaque. This exposes the area to urine passing through the calyces (Andrew P 2010).

The second pathway is due to crystal deposition within the lumen of specific renal tubular segments. These stone formations occur in the ducts of Bellini (BD), also known as the papillary (collecting) duct or in the inner medullary collecting ducts (IMCD). The predominant type of stone formed by this mechanism is a CaP stone. This can be attributed to two factors; firstly, these are the sites of highest CaP supersaturation as the final urine composition is closely monitored in this segment and secondly, due to the increasing alkaline pH of urine in this segment. Note that alkaline urine favours calcium phosphate precipitation while acidic urine favours the precipitation of calcium oxalate (Fredric L. 2010).

The third pathway involves free crystallization in solution. These free stones are predominantly formed in the renal pelvis and composed of cysteine due to its poor solubility. Cysteine is excreted in high amounts in the urine; as such it is a prime candidate for supersaturation. As these stones are not attached to the renal pelvis they are easily washed out during surgeries in comparison to stones that form via the other two mechanisms (Fredric L.2010).

### **1.1.3 Types and causes of kidney stones**

The predominant type of kidney stones are calcium containing (80%). The other types include: uric acid stones, purine stones, ammonium acid urate stones, cysteine stones and struvite stones (Worcester and Coe 2008).

#### **Calcium stones**

Idiopathic hypercalciuria (IH) is the major cause of calcium containing kidney stones. Idiopathic hypercalciuria describes a clinical condition in which the serum calcium level is normal, however the individual produces urine with increased amounts of calcium in it. The exact molecular mechanism mediating IH is not known. It is likely a disease caused by a variety of different factors. As such some persons with IH have been observed to have: increased serum 1,25-dihydroxy vitamin D<sub>3</sub> levels, increased calcium reabsorption from the intestine, decreased renal reabsorption of calcium, decreased bone mineral density, decreased renal phosphate reabsorption along with decreased serum phosphate levels (Worcester and Coe 2008).

Kidney stones can occur in approximately 20% of patients with primary hyperparathyroidism with around 5% forming calcium stones. These patients show slightly increased calcium levels in their serum which is a result of elevated parathyroid hormone (PTH) and low serum phosphorous (Worcester and Coe 2008).

Other non-calcium containing stones include uric acid stones, purine stones, ammonium acid urate stones, cysteine stones and struvite stones (Worcester and Coe 2008).

#### **1.1.4 Associated diseases**

Kidney stones are associated with the occurrence of chronic kidney disease (CKD). CKD in turn is a major risk factor for myocardial infarction (MI) (Rule, Roger et al. 2010). It is reported that patients with stones are at 38% increased risk for MI. Also kidney stones are indirectly associated with other diseases including hypertension, diabetes, obesity, dyslipidemia, gout, alcohol abuse and tobacco abuse (Rule, Roger et al. 2010).

#### **1.1.5 Treatment**

The treatment for kidney stones can be medical or interventional. Medical treatment includes increasing hydration, modification of the diet and potentially treatment of thiazide diuretics (to reduce urinary calcium excretion) (Schissel and Johnson 2011). Stones can pass naturally from the body. Stones that fail to pass often require surgical procedures. These interventional treatments include extra-corporeal shock wave lithotripsy (ESWL) for stones less than 2 cm in size, intracorporeal lithotripsy for large stones and ureteroscopy i.e. examination of the upper urinary tract using an endoscope to diagnose the kidney stones and then the use of laser lithotripsy. This latter treatment involves the use of laser rays to break the kidney stones into small pieces which can easily pass out in the urine (Worcester and Coe 2008).

## **1.2 OSTEOPOROSIS**

### **1.2.1 Prevalence**

Osteoporosis is a skeletal disorder characterized by low bone mineral density and an increased risk of fracture (Samelson and Hannan 2006). The typical fractures of osteoporosis include: fractures of the hip, vertebral body and the distal forearm. In the year 2000, 9 million osteoporotic fractures occurred worldwide. In the United States alone, \$20 billion is spent annually on osteoporotic fractures. Future projections show that the incidence of hip fracture would be a staggering 6.26 million in 2050 (Cole, Dennison et al. 2008). In Canada in the year 2010 the estimated cost to the Canadian health care system for treating fractures in men over the age of 50 years was approximately \$570 million per year. Thus, osteoporosis has a huge impact on the Canadian economy (Tarride, Guo et al. 2012).

### **1.2.2 Pathophysiology**

Human bone comprises two types of tissues, namely cortical (compact) and trabecular (spongy) bone. Osteoporosis affects both these tissues equally. Trabecular bone loss occurs over the entire life span whereas cortical bone loss is related to estrogen deficiency. In women estrogen deficiency is at its peak following menopause. In men the level of bioavailable estrogen decreases with age (Khosla, Melton et al. 2011).

There are two types of osteoporosis, namely postmenopausal (type I) and senile (type II) osteoporosis. Both types are common in women whereas men suffer from type II

osteoporosis exclusively. The major players involved in bone remodeling; a process that when perturbed can cause osteoporosis, are osteoclasts-bone resorbing cells, osteoblasts- bone-forming cells, macrophage colony-stimulating factor (M-CSF) and receptor activator of nuclear factor- $\kappa$ B ligand (RANKL). Osteoprotegerin (OPG) is a decoy receptor of RANKL and antagonizes its action of osteoclasts genesis (Sipos, Pietschmann et al. 2009).

### **1.2.3 Treatment**

The treatment of osteoporosis includes drugs, implants and dietary alterations. Bisphosphonates are the most commonly prescribed drugs for this disorder. (Otomo-Corgel 2000). Bisphosphonates act by decreasing bone resorption (Papapoulos SE 2008). Hormone therapy post menopause has also been used. This therapy is comprised of bazedoxifene (BZA) with conjugated estrogens (CE) (Komm and Mirkin 2012). Dietary changes include increased calcium intake and supplementation with the hormone vitamin D. Further lifestyle alterations to prevent osteoporosis include; smoking cessation, as well as decreased sodium, caffeine and alcohol consumption (Garriguet 2011).

### 1.3 CALCIUM HOMEOSTASIS

Maintaining calcium homeostasis is of absolute importance as calcium is involved in many vital activities including transport of ions over cell membranes, muscle contraction/relaxation, neural networks, the immune system, exocrine/endocrine cell function, blood coagulation and as enzyme cofactors. Also it is a main component of bone (Suzuki, Landowski et al. 2008). A normal individual will excrete approximately 150 mg of calcium per day in their urine (Worcester and Coe 2008).

The three organs that take part in the maintenance of plasma calcium levels are the intestine, kidney and bone. The intestine absorbs calcium from the diet; the kidney regulates urinary calcium excretion by modulating the amount in the ultrafiltrate and the bone stores calcium. The calcium sensing receptor (CaSR) is responsible for sensing changes in the extracellular fluid calcium levels. The CaSR communicates circulating calcium levels to these participating organs. Moreover at least three calcitropic hormones, namely parathyroid hormone (PTH), the active form of vitamin D, 1,25-dihydroxyvitamin D<sub>3</sub>, and calcitonin participate in maintaining circulating calcium levels within a fixed range (2.2- 2.6 mmol/L of total calcium) (Lambers, Bindels et al. 2006). The major source of vitamin D is sunlight. Dietary intake of vitamin D is recommended to be 600 IU (15µg) for people aged <70 years when exposure to sunlight is low (Nowson et al 2012).

The active form of vitamin D is synthesized by dual hydroxylation; first in the liver and then in the kidney (Razzaque M. 2011). PTH regulates the formation of the active

form of vitamin D<sub>3</sub> that in turn controls the expression of the calcium transport proteins including TRPV5 and calbindin-D<sub>28k</sub> in the kidney. When calcium in the plasma decreases, PTH levels increase. This in turn upregulates the renal expression of 1-alpha hydroxylase, an enzyme that catalyzes the conversion of inactive vitamin D<sub>3</sub> to the active form of vitamin D<sub>3</sub>. Increased circulating active vitamin D<sub>3</sub> upregulates the expression of transport proteins prerequisite for the transcellular (re)absorption of calcium from the distal nephron as well as the intestine. When calcium in the blood increases, PTH secretion is inhibited. Active 1,25-dihydroxy vitamin D<sub>3</sub> synthesis is reduced and reabsorption of calcium by the kidney is decreased. Under these circumstances calcitonin is released, which signals to increase bone mineralization (Lambers, Bindels et al. 2006).

## **1.4 CALCIUM FLUX ACROSS THE NEPHRON**

### **1.4.1 Glomerular filtration**

Of the total calcium present in plasma approximately 40% is bound to albumin and other proteins, the remaining 60% exists as free ionized calcium. Only the free calcium is subject to glomerular filtration. Around 99% of filtered calcium is reabsorbed by the nephron (Milica B and Valdivielso JM 2012). In the nephron, 65% is reabsorbed by the proximal tubule, 20% by the thick ascending limb, 10% by the distal convoluted tubule and the connecting tubules and less than 5% by the collecting ducts. The remaining amount is excreted in the urine.

### **1.4.2 Paracellular vs Transcellular Transepithelial Reabsorption**

Paracellular transport is the transport of ions through the tight junction between two cells. The tight junction strands form a mesh like structure in which the tight junction proteins are embedded. This transport pathway is passive in nature (García, Ramsey et al. 1998). Consequently flux through this pathway is driven by the electrochemical gradient. There are three types of tight junction proteins that mediate paracellular transport directly or indirectly. They are membrane-spanning proteins that include the claudins, occludin and junctional adhesion molecules; scaffolding proteins such as zona occludens and signaling molecules, for example transcription factors and kinases/phosphatases. The membrane-spanning proteins are directly involved in the transport mechanism while scaffolding proteins form a link between the membrane-spanning proteins and the actin cytoskeleton. Signaling molecules are involved in tight

junction protein transcription and expression (Li, Ananthapanyasut et al. 2011)  
**(Figure 1.1).**

Transcellular ion flux is the movement of ions through epithelial cells. This is an active transport process (Kawedia, Nieman et al. 2007). The whole transport process takes place via three major steps. First, transport must occur across the luminal membrane. Second, movement occurs across the cytosol and third and finally, transport across the basolateral membrane. The energy for this active process could be in the form of an energy-providing reaction like ATP-hydrolysis or in the form of an electrochemical potential difference (Murer, Ahearn et al. 1983).

**Figure 1.1** Schematic representation of paracellular and transcellular reabsorption along the nephron

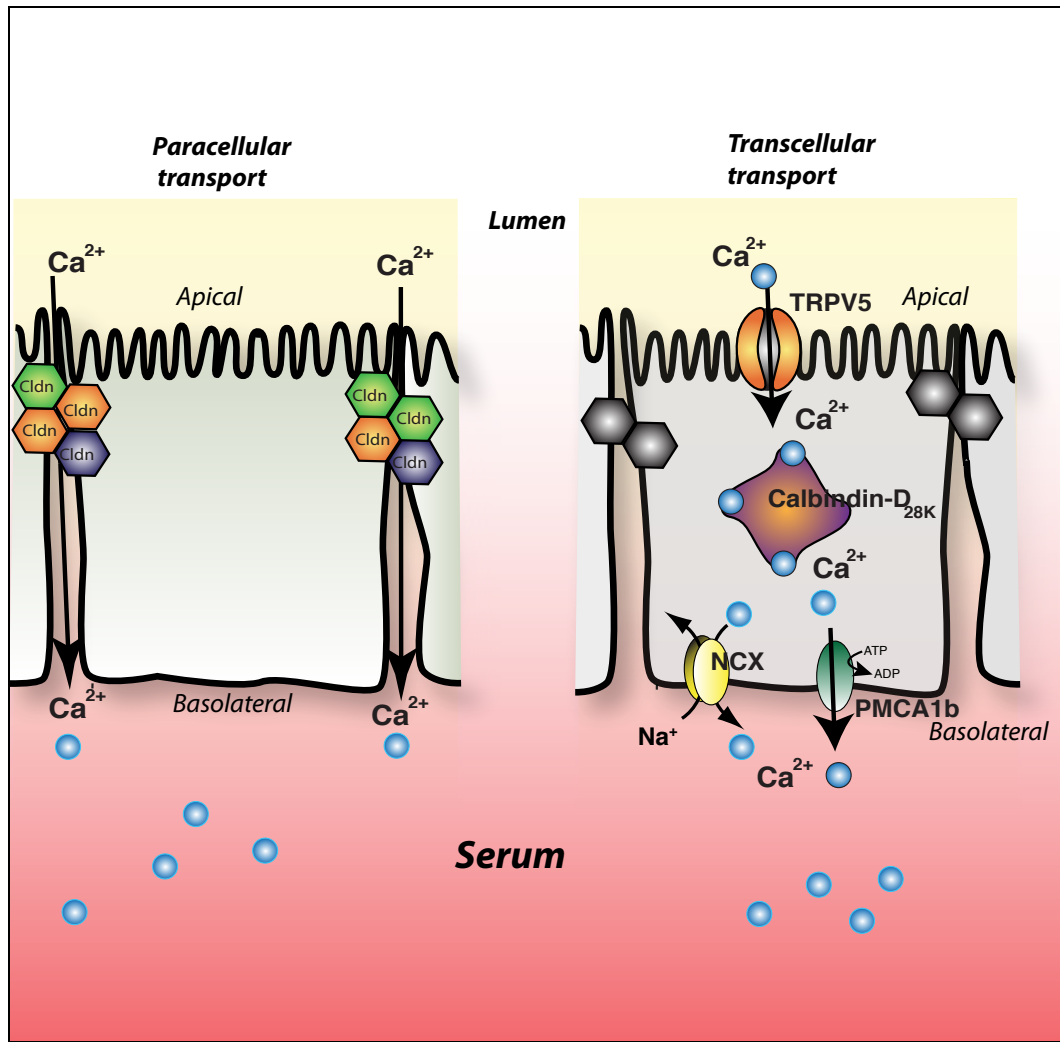


**Figure 1:** Schematic representation of paracellular and transcellular transport across the nephron. Passive paracellular transport occurs via the tight junction proteins between cells. Active transcellular transport occurs through the cell and is carried out via membrane proteins.  $\text{Ca}^{2+}$  -calcium ions,  $\text{Na}^+$  -sodium ion, Cldn- claudins (tight junction proteins), TRPV5- transient receptor potential vanilloid 5 receptor, NCX- sodium calcium exchanger and PMCA1b- plasma membrane calcium ATPase.

### **1.4.3 Calcium flux across proximal tubule**

In the proximal tubule calcium flux occurs paracellularly through the tight junction. It is reported that calcium transport is relative to sodium and water transport in this nephron segment (Suki 1979). The driving force here is the chemical and electrical gradient (Fedric C 1980) generated by active transcellular sodium flux across the proximal tubule. The chemical gradient is generated by removal of water thereby concentrating  $\text{Ca}^{2+}$  in the lumen. The second mechanism resulting in paracellular  $\text{Ca}^{2+}$  flux across this nephron segment is solvent drag, or convection, whereby the water flux drives passive paracellular calcium flux (Pan, Borovac et al. 2012). The potential difference (PD) across the proximal tubule depends on the luminal glucose, amino acids and bicarbonate (Kokko P. 1973). The PD is segment specific and changes with the changing concentration of the solutes. Studies on rat proximal tubule show that the first part (0.1 to 0.3 mm of tubular length) of the proximal tubule has a PD of approximately -1.5 mV lumen negative. The second segment of proximal tubule (1mm of tubular length) shows a lumen positive PD of 2 mV. The PD falls to 1.6 mV in the last loop of the proximal tubule (Fromter and Geßner 2001).

### **1.4.4 Calcium flux across thick ascending limb (TAL)**

Calcium flux across the thick ascending limb of the loop of Henle occurs via the paracellular pathway. This process is dependent on the tight junction proteins claudin-16 and claudin-19. It has been shown that claudin-16 and claudin-19 interact with each other at the tight junction strands to form a cation selective pore that mediates  $\text{Ca}^{2+}$  reabsorption. The predominant driving force is the lumen positive transepithelial

diffusion potential generated due to transepithelial NaCl reabsorption from the TAL via NKCC2 and Na/K-ATPase (Hou, Renigunta et al. 2008). Although the concentration gradient here also favours Ca<sup>2+</sup> reabsorption.

#### **1.4.5 Calcium flux across distal nephron**

In the distal nephron (Distal convoluted tubule (DCT), Connecting tubules (CNT) and in some species Collecting ducts (CCD) (Bindels, Hartog et al. 1991) calcium flux occurs via the transcellular pathway. The main players involved are transient receptor potential vanilloid 5 (TRPV5), calbindin-D<sub>28k</sub>, sodium-calcium exchanger 1 (NCX1) and plasma membrane calcium ATPase1b (PMCa1b). TRPV5 is expressed in the apical membrane of the cell. It allows for selective calcium entry into the cell (Suzuki, Landowski et al. 2008). An inward electrochemical gradient also plays a role in the entry of calcium into the cell. Once inside the cell, calcium binds to calbindin-D<sub>28k</sub> that then ferries it to the other side of the cell. NCX1 and PMCa1b act to extrude calcium back out of the cell across the basolateral membrane into the blood (Lambers, Bindels et al. 2006).

## 1.5 CLAUDINS

### 1.5.1 Structure and Function

Claudins are a family of tight junction proteins, which contains 27 known isoforms in humans. They are 20-27 kDa in size and have 4 transmembrane domains. Both their amino- and carboxy- terminus is in the cytoplasm (Balkovetz 2006). They have 2 extracellular loops that face the paracellular space. Expression of claudins varies according to organ and organism (Li, Ananthapanyasut et al. 2011). In the nephron their expression and distribution is segment specific (Gunzel, Stuiver et al. 2009).

Claudins have been reported to play a role not only in renal epithelial cells but also in the epithelia of the intestine, retina, cochlea, cancer, blood-brain barrier etc. In the kidney, based on claudin –claudin interaction they can act as a paracellular barrier or a pore. Their function can be studied by measuring the transepithelial resistance (TER) they confer when over expressed in renal epithelial cell culture models. Chimera and mutagenesis studies have shown that claudin (Cldn)-1, -4, -5, -8, -9, -11, -15 and -19 act as paracellular barriers while claudin-2 and -16 act as a pore. Colegio *et. al.* showed that the first extracellular loop of a claudin is responsible for its barrier/pore forming function (Colegio et al. 2002).

Van Itallie reported that in the Madine-Darby canine kidney (MDCK) cell line some claudins form a pore of approximately 4 Å in size (Van Itallie et al. 2008). Other studies by Yu et al. have reported the pore size of Cldn2 to be 6.5 Å (Yu et al.2009). The charge selectivity of the pore depends on the electrostatic interaction of the ions

with a charged site within the claudin pore itself, this appears to be conferred by the first extracellular loop (Li, Ananthapanyasut et al. 2011).

## **1.5.2 EXPRESSION, FUNCTION AND MUTATIONS IN CLAUDINS**

We will provide some specific details of claudins central to our studies and calcium homeostasis below. A detailed review of each claudin is not presented.

### **1.5.2.1 Claudin- 2 (Cldn2)**

Cldn2 is expressed in liver, kidney, gut and pancreas. In the mouse nephron it has been shown by immunofluorescence that Cldn2 is present in: Bowman's capsule, the proximal tubule and the thin descending limb of Henle's loop (Kiuchi-Saishin, Gotoh et al. 2002). The Cldn2 pore is not permeable to uncharged molecules >182 Da. This pore demonstrates a selective permeability sequence in the order of  $K^+ \approx Na^+ > NMDG^+ > choline^+ \gg Cl^- = Br^-$  in MDCK cells. This data indicates that Cldn2 is cation selective. Expression of Cldn2 decreases transepithelial resistance (Amasheh, Meiri et al. 2002).

Cldn2 plays a critical role in calcium absorption from the intestine (Fujita, Sugimoto et al. 2008). Tamura et al have shown that in the Cldn2 knockout mouse,  $Na^+$  homeostasis is unaltered, however Cldn15 deficient mice demonstrate significant alterations in  $Na^+$  homeostasis and are in fact  $Na^+$  deficient (Tamura, Hayashi et al. 2011). Importantly, knockout of Cldn2 in mice causes a loss of cation ( $Na^+$ ) selectivity in the proximal tubule and hypercalciuria (Muto, Hata et al. 2010).

### **1.5.2.2 Claudin-10 (Cldn10)**

There are two isoforms of Cldn10, Cldn10a and Cldn10b. Cldn10b is 2 amino acids larger than Cldn10a. Though these isoforms are quite similar to each other they differ in their charge on the first extracellular loop. Cldn10a has seven positively charged and two negatively charged amino acids whereas Cldn10b has 4 positive and 5 negative charges in the first extracellular loop. Cldn10a is expressed specifically in the kidney while Cldn10b is present in almost all epithelial tissues. It has been demonstrated in MDCK-II cells and in LLC-PK1 cells that expression of Cldn10a causes an increase in Cl<sup>-</sup> permeability and expression of Cldn10b causes an increase in Na<sup>+</sup> permeability (Gunzel, Stuiver et al. 2009).

### **1.5.2.3 Claudin-12 (Cldn12)**

Cldn12 is expressed in the duodenum, jejunum, ileum and colon of the intestine (Fujita, Chiba et al. 2006). Cldn12 along with Cldn2 were reported to be involved in calcium absorption along the intestine (Fujita, Sugimoto et al. 2008). Whether Cldn12 is expressed in the kidney or not has not yet been determined.

### **1.5.2.4 Claudin- 14 (Cldn14)**

Recently the expression of Cldn14 was reported in the thick ascending limb (Gong, Renigunta et al. 2012). Earlier Cldn14 was reported to be present in the distal convoluted tubule (Kirk, Campbell et al. 2010) and in the proximal tubule (Ben-Yosef, Belyantseva et al. 2003). A genome wide association study (GWAS) has related

sequence variants in the Cldn14 gene with kidney stones and bone mineral density (Thorleifsson, Holm et al. 2009). Mutations in the Cldn14 gene have been associated with nonsyndromic recessive deafness DFNB29 (Wilcox, Burton et al. 2001).

#### **1.5.2.5 Claudin-16 (Cldn16)**

Cldn16 is expressed in the thick ascending limb (TAL) (Ikari, Okude et al. 2008). Cldn16 has 10 negative residues in its first extracellular loop that are responsible for the charge selectivity of the pore it forms. Studies have shown that Cldn16 has preferential selectivity towards divalent cations (Colegio, Van Itallie et al. 2002). Mutations in Cldn16 have been reported in patients with familial hypomagnesemia with hypercalciuria and nephrocalcinosis (FHHNC). Some FHHNC mutations result in the disruption of the localization of Cldn16. Specifically they cause the relocalization of Cldn16 from the tight junction to lysosomes. This change of localization interferes with the ability of Cldn16 to conduct the paracellular flux of calcium and magnesium (Ikari, Okude et al. 2008).

#### **1.5.2.6 Claudin- 19 (Cldn19)**

Cldn19 is expressed in the TAL and is known to be involved in the paracellular flux of calcium and magnesium. It plays a role in the pathogenesis of FHHNC. Hou *et al.* showed that Cldn16 and Cldn19 interact with each other in the TAL. Co-expression of Cldn16 and Cldn19 resulted in cation selectivity of LLC-PK1 cells. Individually Cldn19 acts as a Cl<sup>-</sup> blocker. Mutations in either Cldn16 or Cldn19 cause FHHNC by disrupting the synergistic effect of these claudins (Hou, Renigunta et al. 2008).

## 1.6 HYPERCALCIURIA

Hypercalciuria is defined as the excessive excretion of calcium in the urine. Idiopathic hypercalciuria can be divided into one of three types i) Absorptive hypercalciuria due to increased intestinal calcium absorption, ii) resorptive hypercalciuria due to increased loss of bone leading to increased urinary calcium and iii) renal-leak hypercalciuria with defective renal calcium reabsorption (Bushinsky and Favus 1988), (Worcester and Coe 2008). Interestingly there is often considerable overlap between the types of hypercalciuria in a single patient suggesting that this division of types is less than adequate. Absorptive hypercalciuria can further be divided into two types, absorptive hypercalciuria I (AH-I) and absorptive hypercalciuria II (AH-II). Patients with AH-I have normocalcemia, hypercalciuria, intestinal hyperabsorption of calcium and normal or decreased values of PTH in the serum and urinary cyclic adenosine 3', 5' monophosphate (Pak, Sakhaee et al. 2011).

Idiopathic hypercalciuria is reported to be 8 times more prevalent in stone forming patients than in normal individuals and is a major risk factor (Luyckx, Leclercq et al. 1999). In patients with IH, 1,25-(OH)<sub>2</sub>D<sub>3</sub> levels are often increased along with an increased expression of the vitamin D receptor (VDR). Dietary components like sodium, proteins, glucose, sucrose and alcohol are also known to play a role in increased urinary calcium excretion and may exaggerate the phenotype of an individual with the disease.

Dent's disease is the best-studied genetic disease with hypercalciuria as part of its phenotype. It is due to a defect in chloride channel 5 (CLC5). The actual genetic defect in IH has not been clearly elucidated. Several candidate genes including: vitamin D receptor (VDR), TRPV5, CaSR and sodium phosphate co-transporter 2 (NPT2) have been screened to study their involvement in IH. There is some evidence that the VDR and CaSR may be abnormal in some individuals with IH, although this has not been clearly delineated. The recent discovery of a gene related to chronic kidney disease called klotho (KI) has also been implicated in IH. Klotho is an anti-aging gene that colocalizes with TRPV5. Klotho deficient mice have decreased expression of TRPV5 and reduced calcium reabsorption (Alexander, Woudenberg-Vrenken et al. 2009). Fibroblast growth factor 23 (FGF23) is a hormone that plays a role in reducing renal tubular phosphate reabsorption and vitamin D synthesis. Klotho acts as a cofactor for FGF23 and their absence may cause IH (Torres, Prie et al. 2007). Another gene known to be indirectly involved in IH is leptin. Leptin acts on the proximal tubules and affects the production of  $1\alpha$ Hydroxylase, an enzyme that converts inactive vitamin D<sub>3</sub> to the active form of vitamin D<sub>3</sub>. Thus leptin indirectly affects renal calcium reabsorption and can cause hypercalciuria (Matsunuma and Horiuchi 2007).

Worcester *et al.* studied calcium flux across the proximal tubule in 12 patients with idiopathic hypercalciuria and calcium containing stones (IHSF). They demonstrated that defective sodium reabsorption from the proximal tubule in patients with IHSF leads to reduced calcium reabsorption resulting in higher luminal Ca<sup>2+</sup>. The excessive

luminal sodium gets reabsorbed in the later part of the nephron. However the kidney fails to reabsorb the excessive luminal calcium resulting in increased excretion of calcium in the urine. This study suggests that idiopathic hypercalciuria is due to defective proximal tubular sodium reabsorption (Worcester, Coe et al. 2008).

## **1.7 THESIS HYPOTHESIS**

We hypothesize that specific claudins are involved in paracellular calcium flux across the proximal nephron

## **1.8 THESIS OBJECTIVES**

1. To identify the claudins expressed in the proximal nephron
2. To determine whether claudin expression is altered by perturbations in calcium homeostasis

**CHAPTER 2**

**MATERIALS AND METHODS**

## **2.1 Animals**

FVB/N (Taconic Farms, Hudson, NY, USA) wild type mice between 8-10 weeks of age were used for all experiments. The experimental protocol for all animal experiments carried out was approved by the Animal Care and Use Committee (ACUC) for Health Sciences at the University of Alberta. This committee abides by the rules and regulations of the Canadian Council on Animal Care (CCAC).

## **2.2 Isolation of whole kidney and proximal tubule RNA**

Wild type mice were euthanized by an intraperitoneal injection of pentobarbital (50 mg/Kg) and kidneys removed and snap frozen in liquid nitrogen. These kidneys were then stored at -80°C until further use.

Proximal tubules were microdissected using a dissection microscope (Olympus America, Inc. Szx16, Center Valley, PA, USA). Dissection procedure was carried out at room temperature. Dissected proximal tubules, or whole kidneys after mechanical disruption, were immediately transferred into RLT buffer on ice from the RNeasy Plus kit (Qiagen, Toronto, ON, Canada) and RNA was isolated as per the manufacturer's protocol and quantified using a spectrophotometer (Nanodrop 2000c, Thermo Scientific, Asheville, NC, USA).

## **2.3 Genomic DNA Isolation (gDNA)**

Whole kidney was digested overnight in a water bath at 56°C using digestion buffer (1M Tris pH 8.0, 0.5M EDTA pH 8.0, 5M NaCl and 20% SDS) and proteinase K

(Invitrogen, Carlsbad, CA, USA). The sample was ground, vortexed vigorously and then chilled on ice for 5 mins. 5M NaCl was next added, the solution mixed, left on ice for 5 mins and then centrifuged at 14,000 rpm at 4°C for 10 mins. DNA was precipitated using ice-cold isopropanol. A pellet was obtained, washed with ice-cold 70% ethanol and centrifuged at 14,000 rpm, 4°C, for 15 mins. The pellet was air dried and finally resuspended in autoclaved ddH<sub>2</sub>O.

#### **2.4 Complimentary DNA (cDNA) synthesis**

1µg of isolated mRNA from proximal tubules or whole kidney, 3 µg/µl of random hexamers (Invitrogen, Carlsbad, CA, USA) and RNase free water was added together and incubated at 70°C for 10 mins. Next, 5X buffer provided with SuperScript II (SSII) (Invitrogen, Carlsbad, CA, USA), 0.1M DTT (Invitrogen, Carlsbad, CA, USA), 25µM dNTP (Invitrogen, Carlsbad, CA, USA), 40U/µl RNase Out (Invitrogen, Carlsbad, CA, USA) 1µl SSII (Invitrogen, Carlsbad, CA, USA) were added to the mixture and incubated at 40°C for 1 hour on a C1000 Thermal cycler (BioRad, Mississauga, ON, Canada) to produce cDNA.

#### **2.5 Negative control for cDNA synthesis (noRT)**

1µg of isolated mRNA from proximal tubules or whole kidney, 3 µg/µl of random hexamers (Invitrogen, Carlsbad, CA, USA) and RNA free water was added and incubated at 70°C for 10 mins. Then, 5X buffer (Invitrogen, Carlsbad, CA, USA), 0.1M DTT (Invitrogen, Carlsbad, CA, USA), 25µM dNTP (Invitrogen, Carlsbad, CA, USA) and 40U/µl RNase Out (Invitrogen, Carlsbad, CA, USA) were added to the

mixture and incubated at 40°C for 1 hour on a C1000 Thermal cycler (BioRad, Mississauga, ON, Canada) to generate the negative control.

## **2.6 Determination of Gene Expression by Polymerase chain reaction (PCR)**

To determine whether a gene was expressed in either whole kidney or isolated proximal tubule, we employed PCR against a specific sequence within the mRNA or cDNA isolated as described above. To this end, 100ng of template (either gDNA, cDNA or noRT) 10X buffer (Invitrogen, Carlsbad, CA, USA), 50mM MgCl<sub>2</sub> (Invitrogen, Carlsbad, CA, USA), 10mM dNTP (Invitrogen, Carlsbad, CA, USA), 20µM of forward and reverse primer (Integrated DNA Technologies Inc, San Diego, CA, USA) and 5U/µl of *Taq* polymerase (Invitrogen, Carlsbad, CA, USA) were mixed together. The PCR reaction (94°C for 1 min, 94°C for 30 seconds, primer melting temperature for 30 seconds, 72°C for 1 min, 35-40X cycles, 71°C for 10 mins and 4°C forever) was carried out with a C1000 Thermal cycler (BioRad, Mississauga, ON, Canada). The subsequent sample was run out on 1.5% agarose gel and visualized with ethidium bromide.

### **2.6.1 Expression primers**

All the primers were designed using the software primer-BLAST (National center for biotechnology information, Bethesda, MA, USA). All primers were synthesized by IDT (Integrated DNA Technologies Inc, San Diego, CA, USA). The sequences are listed in table 2.1. Note, for all reactions except the sodium phosphate cotransporter

Iic (NaPiIic), the primers targeted a single exon, thus permitting the detection of the same size band in both genomic DNA (gDNA) and cDNA.

**Table 2.1. Primers used to detect expression by PCR**

	<b>Sequence</b>
Claudin 1	Forward: CACCGCCTACCCGGACCAGA Reverse: TTCCA CTGGGGCAGGGCAGT
Claudin 2	Forward: GCATTGTGACGGCGGTTGGC Reverse: GTGGCAAGAGGCTGGGCCTG
Claudin 3	Forward: GTGCGAGCCCCAGGAGAGGA Reverse: ATGAAGGCCGAAACGCGCCA
Claudin 4	Forward: AGCACAGGTCAGATGCAGTG Reverse: GTCTCGTCCTCCATGCAGTG
Claudin 5	Forward: GCTCTCAGAGTCCGTTGACC Reverse: CTGCCCTTTCAGGTTAGCAG
Claudin 6	Forward: TGCTTGGCTGGGTCAACGCC Reverse: GCCCAGGTAGAGGGAGGCC
Claudin 7	Forward: CTGCAACTGCTGGGCTTTTCAATGG Reverse: TCCATCCAGAGCCCCTTGTACATGG
Claudin 8	Forward: TGCAAGGTCTACGACTCCCT Reverse: GTGCACTTCATTCCGAGGAT
Claudin 9	Forward: GCCCGCAGCTGTGAGGTCTG Reverse: GGGCCTTGGCACCTTCGTCC
Claudin 10a	Forward: GCAGGCAAGGCTGAGCGACA Reverse: GCCTTGGAAGGACTATCGTGAGGACA
Claudin 10b	Forward: GCTGGTGAGGCCAAGGTGCC Reverse: TGCAGGGCTGGCCTCAGGAA
Claudin 11	Forward: CGTGGGTTGGATTGGCATCATCGT Reverse: AGACCAGTGGCCATGACGCAG
Claudin 12	Forward: TGTGCGAGGCCTCTTTGCGG Reverse: CCACAGGCCCGTGTAATCGTCA
Claudin 13	Forward: TCATACGTGCTGGCCCCCGA Reverse: TGGCACCCACCAACCCAGT
Claudin 14	Forward: TGGCGCTGCCCCGGGATCT Reverse: TGGTAGCTCCGGCCCTGGAC
Claudin 15	Forward: GGCCAAAGCCCCGGAATTCA Reverse: CTCCAGTAGCTGTTTGAAAGGGTCAA
Claudin 16	Forward: CGTGAAAGACTGGGCACTATCATCCC Reverse: AGTCTGTCCAGGTGGCCACGA
Claudin 17	Forward: CGGTACTGGAAGCAGCGCGT Reverse: TGTGGCACGCGGTATGCAGG
Claudin 18	Forward: AGCCCTGATGATCGTGGGCATT Reverse: TCATCTTGGCCTTGGCAGAGTCAT
Claudin 19	Forward: CCGCCGCTGTCGCTCCTTTA Reverse: AACTGAGCGTCGTTATCACACGAA
Claudin 20	Forward: TGGCCTCGGCAGGTCTCCAG Reverse: GCACATGGACGGGGAGCGAC
Claudin 22	Forward: CAGGCGGCTGCACTTCTGCT Reverse: CACCGTCTTGTGGGCCACCC

**Table 2.1 continued..**

Claudin 23	Forward: TGCTGCTTCTGGGCGGCTTC Reverse: AGGAGGCCGATGCTGTCCGT
$\beta$ Actin F	Forward: CCCTCCATCGTGCACCGCAA Reverse: GACTCAGGGCATGGACGCGA
GAPDH	Forward: TTGGCCGTATTGGGCGCCTG Reverse: TCGGCCTGACTGTGCCGTTG
TRPV5	Forward: CAGACCCCAGTGAAGGAGCTGGT Reverse: ATCTCGGAACTTGAGGGGGCGG
Occludin	Forward: CGGCCGATGCTCTCTCAGCC Reverse: GGCTGCCATGGCCAACAGGA
Tricellulin	Forward: GCAGCAGGCACCTCCAGGTC Reverse: ATGGGACACGCGCCTCTGAT
JAM1	Forward: CCCCTCCTCTGTCACCATTGGGA Reverse: CCGGGTTTTCTTGGCATCTGCTGT
NaPi 2a	Forward: ACGGGCTACCTACACCATGTCACC Reverse: GAACACGGAGCTGCTCTGGACAAC

**Table 2.1:** Primer sequences used for detection of claudins and other proteins by polymerase chain reaction; GAPDH- Glyceraldehyde-3-phosphate dehydrogenase, JAM1- Junction adhesion molecule 1.

## **2.7 Gel Electrophoresis**

A 2% (2g in 100ml) agarose (Invitrogen, Carlsbad, CA, USA) gel was prepared in 1X TAE buffer (0.04M Tris-acetate and 0.001M EDTA) and heated at full power in a microwave (Danby, Guelph, ON, Canada) for 2 mins. The solution was allowed to cool sufficiently and 2 $\mu$ l of ethidium bromide (Sigma-Aldrich Canada Ltd., Oakville, ON, Canada) was added. The gel was casted in a gel electrophoresis apparatus (Electrophoresis system, Fisher Scientific Company, Ottawa, ON, Canada) and allowed to solidify. To all the samples, 2.5 $\mu$ l of 2X loading dye (Fermentas Canada Inc, Burlington, ON, Canada) was added and mixed uniformly. All the samples along with a 100bp DNA ladder (Generuler, Fermentas Canada Inc, Burlington, ON, Canada) were loaded on the gel and run at a current of 140 volts for 40 mins (Power Pca 200, BioRad, Mississauga, ON, Canada). The gel was viewed with a gel imager (Gel Doc EZ Imager, BioRad, Mississauga, ON, Canada).

## 2.8 Animal experiments

### 2.8.1 Experimental protocol 1 – altered calcium diets

FVB/N mice (Taconic Farms, Hudson, NY, USA) were fed a low (0.01%, TD.95027), normal (0.6%, TD.97191), or high (2%, TD.00374) Ca<sup>2+</sup> diet for either 10 or 21 days, respectively (n=48, 8 in each group). Diets were custom made by Harlan Laboratories (Madison, WI, USA). Mice were housed in metabolic cages at the end of the experimental period. On the last day, animals were anesthetized using pentobarbital and blood was withdrawn by perforating the orbital vessels and used to *i*) measure blood gas/electrolytes- sodium, potassium, ionized calcium, hematocrit, Hb, glucose, pH, pCO<sub>2</sub>, pO<sub>2</sub>, bicarbonate and SO<sub>2</sub> (with a VetScan i-STAT 1 Analyzer, Abaxis, Union city, CA, USA) and *ii*) processed into serum. To isolate serum, blood was collected in a borosilicate glass tube (disposable culture tubes, Fisher Scientific Company, Ottawa, ON, Canada) and allowed to coagulate overnight at 4°C. The next day the tubes were centrifuged at 14000 rpm to separate serum from clot (Microfuge 22R centrifuge, Beckman Coulter Canada, Inc., Mississauga, ON, Canada). The kidneys were removed and snap frozen in liquid nitrogen. All experimental procedures were approved by the Animal Care & Use committee for Health Sciences at the University of Alberta (Protocol #576).

### 2.8.2 Experimental protocol 2 - vitamin D<sub>3</sub> administration

FVB/N mice were placed on a standard diet with *ad libitum* access to food and water. Active vitamin D, 1,25(OH)<sub>2</sub> vitamin D<sub>3</sub> (1,25(OH)<sub>2</sub>D<sub>3</sub>) (Sigma-Aldrich, Oakville, ON, Canada) was dissolved in absolute ethanol and diluted to 5% in phosphate-

buffered saline. Animals received 1,25(OH)<sub>2</sub>D<sub>3</sub> (500 pg/g bodyweight, n=8) or vehicle (n=8), by intraperitoneal injections for 5 days. During the last 48 hrs of the experimental period, mice were placed in metabolic cages. Otherwise, mice were maintained and processed exactly as described in experimental protocol 1.

### **2.8.3 Experimental protocol 3 – cinacalcet treatment**

FVB/N mice (n=12) were given Cinacalcet (Sensipar®, Amgen, CA, USA) in food at a dose equivalent to 1mg/g bodyweight or vehicle. The mice were maintained on a standard diet with *ad libitum* access to food and water. Animals were kept in regular cages for 2 days and subsequently placed in metabolic cages for the remaining 4 days of the study. The mice were then processed essentially as described in experimental protocol 1.

## **2.9 Determination of solutes, creatinine, and hormones**

### **2.9.1 Urinary calcium**

Total Ca<sup>2+</sup> in urine was determined using a colorimetric assay kit (Quantichrom TM Ca<sup>2+</sup> Assay Kit, BioAssay System, Hayward, CA, USA) as per the manufacturer's protocol. In brief, standards and samples were pipetted into a 96-well plate. Working reagent was added and the plate was incubated for 3 mins at room temperature. Absorbance was measured at 570-650 nm using a monochromator-based microplate reader (Synergy Mx, Biotek, USA).

### **2.9.2 Urinary creatinine**

Urinary creatinine was measured using the Creatinine Parameter Assay Kit (R&D Systems Inc., Minneapolis, MN, USA). All samples, standards and controls were prepared as per the manufacturer's protocol. To each well containing the standard, control or the sample, alkaline picrate solution was added and the 96-well plate was incubated for 30 mins at room temperature. The optical density of each well was measured at 490nm using a monochromator-based microplate reader (Synergy Mx, Biotek, city, state, USA).

### **2.9.3 Plasma PTH Assay**

Intact plasma PTH levels were determined with a mouse PTH ELISA kit (Immutopics International, San Clemente, CA, USA) as per the manufacturer's protocol. In brief PTH standards, controls and samples were added in duplicates to a Streptavidin coated plate. Then a working antibody solution (equal volumes of mouse intact PTH

biotinylated antibody and mouse intact PTH HRP conjugated antibody) was added and the plate incubated on a rotator for 3 hours in the dark. Each well was washed 5 times with working wash solution. Next, ELISA HRP substrate was added and the plate was incubated on a rotator for 30 mins in the dark at room temperature. The plate was finally read at 595nm after ELISA stop solution was added. The absorbance was read at 450nm using a monochromator-based microplate reader (Synergy Mx, Biotek, USA).

#### **2.9.4 1,25- Dihydroxy Vitamin D Assay**

Serum 1,25(OH)<sub>2</sub>D<sub>3</sub> concentrations were determined by a  $\gamma$ - radioimmunoassay (RIA) kit (Immunodiagnostic Systems Ltd., Fountain Hills, AZ, USA). First, samples were immunoextracted as per the manufacturer's protocol. To all the samples (60 $\mu$ l), controls, standards and non-specific binding (NSB) count, assay buffer (160 $\mu$ l) was added in duplicate in glass tubes. Sheep-anti-vitamin D primary antibody was then added to all tubes except NSB and incubated overnight at 4°C. All samples were next labeled with <sup>125</sup>I-vitamin D and incubated for 2 hours at room temperature. Sac-cel was added to the solution and then a pellet was obtained by centrifugation at 10°C for 10 mins at 3500 rpm which was later washed with wash solution. The samples were then dried and the radioactivity measured using a gamma counter (Cobra II Auto Gamma, Canberra Packard, Meriden, CT, USA).

## **2.10 Real-time PCR**

### **2.10.1 RNA isolation**

Total mRNA was isolated from kidney using TRIzol Reagent (Invitrogen, Carlsbad, CA, USA) as per the manufacturer's instructions. Half a snap frozen kidney was homogenized in ice-cold TriZol and to the supernatant chloroform (Invitrogen, Carlsbad, CA, USA) added. The aqueous phase was separated and then mixed with isopropanol after which it underwent centrifugation at 4°C, 12000g for 15 mins. The pellet obtained was washed with 70% ethanol and then air-dried. The pellet was next dissolved in RNase free water and 10X DNase buffer and DNase added. RNA was precipitated using an ice-cold phenol:chloroform (1:1) mixture. 3M NaAC pH5.2 and 100% ethanol were then added to the RNA after which it was incubated overnight at -20°C, or for 2 hours at -80°C. The solution was centrifuged and the pellet was washed in 70% ethanol before air-drying. This pellet was dissolved in RNase free water and the concentration determined using a spectrophotometer (Nanodrop 2000c, Thermo Scientific, Asheville, NC, USA).

### **2.10.2 Quantitative PCR**

Isolated total mRNA was reverse transcribed into cDNA as detailed above. 5µl (500ng cDNA) was used as template to determine the gene expression of claudin-1, -2, -3, -8, -10a, -12, -15, -16 and -19. A mixture consisting of TaqMan universal qPCR master mix (Applied Biosystems Inc, Foster City, CA, USA), primer, probe and RNase free water was prepared and added to the cDNA in a 96-well plate (Sarstedt Inc, Montreal, QC, Canada). As an internal control mRNA levels of the housekeeping gene 18S

Ribosomal RNA were determined. Expression levels were quantified with an ABI Prism 7900 HT Sequence Detection System (Applied Biosystems Inc, Foster City, CA, USA). Primers and probes were made by IDT (Integrated DNA Technologies Inc, San Diego, CA, USA) or ABI (Applied Biosystems Inc, Foster City, CA, USA). The sequences of all primers and probes utilized are listed in table 2.2. 18S was chosen for normalization of RNA obtained from each kidney sample. We choose 18S as none of the experimental perturbations resulted in a significant change in its expression (Cat # Mm03928990\_g1).

**Table 2.2. Real- time PCR primers and probes**

	<b>Sequence</b>
Claudin 1	Forward: TGGTGTGGGTAAGAGGTTG Reverse: GAATTCTATGACCCCTTGACCC Probe: CTACTTTCCTGCTCCTGTCCCCG
Claudin 2	Forward: GCTTGTGACCCCTTGAC Reverse: CTCCTTACAAGTATCTGTGGGTG Probe: CGTTCGCCTTTCTCTGGACCTAGT
Claudin 3	Forward: CACCAAGATCCTCTATTCTGCG Reverse: GGTTTCATCGACTGCTGGTAG Probe: CCCCTCAGACGTAGTCCTTGCG
Claudin 8	Forward: AGCTGGATAACAATTTGGGAGG Reverse: CCACTGAGGCATGATAGTCAC Probe: TGCAGCCATTTGAAGAGCGTAGGT
Claudin 10a	Forward: GCTTCTCTTGCATCATTGGG Reverse: AAATCTCCTTCTCCGCCTTG Probe: CGTGGGTCCGTTGTATGTGTAGCC
Claudin 12	Forward: TCGCCAGAACGCACTTC Reverse: TGAAGTCAGATGCAACAGGAG Probe: ATCCCGCTCACCCACTCCG
Claudin 14	Forward: TGGCATGAAGTTTCAAATCGG Reverse: CGGGTAGGGTCTGTAGGG Probe: TGAGAGACAGGGATGAGGAGATGAAGC
Claudin 15	Forward: CTTCCCTACAAGCCTTCTACG Reverse: AGACAGTGGGACAAGAAATGG Probe: AGCTGATGTCACCTCTCATCCGAGGT
Claudin 16	Forward: AGACTGTTGGATGGTGAACG Reverse: AGCTTCAAGGGATGTTCTGC Probe: CGCTTTTGATGGGATTCTGAACCTGC
Claudin 19	Forward: AAGGGCTGTGGATGTCTTG Reverse: CTCGTGCTGACTGGATATGAC Probe: AGGGCCAGGAGTGAATCGTAGAGT

**Table 2.2:** Real-time PCR primer and probe sequences used for detection of mRNA levels of claudins

## 2.11 Immunostaining

Kidney sections (10µm) were cut from kidneys that had been fixed in PLP (0.5-2.0% Paraformaldehyde, 0.01M Na-m-periodate, 0.075M Lysine-HCl and 0.038M Phosphate-buffer, pH 7.4) and then snap frozen in liquid nitrogen. Heat induced epitope retrieval was carried out on the sections using target retrieval buffer (0.01M Sodium citrate and 0.01M citrate, pH 6.0). The sections were washed in TN buffer (0.1M Tris/HCl pH 7.6 and 0.15M NaCl) and incubated in 0.3% hydrogen peroxide in TN buffer for 30 mins. Again the sections were washed in TN buffer and then blocked for 30 mins in TNB buffer (0.1M Tris/HCl pH 7.6, 0.15M NaCl and 0.5% Blocking reagent- provided in the kit). The sections were incubated overnight at 4°C in primary antibody (1:200 in TNB). The sections were then washed in buffer TNT (0.1M Tris/HCl pH 7.6, 0.15M NaCl and 1% TritonX 100) and incubated with secondary antibody (1:2000 in TNB) and 4',6-diamidino-2-phenylindole (DAPI) for 1 hour at room temperature. Finally the sections were washed in TNT buffer and the slides mounted with DAKO (DAKO Canada Inc, Burlington, ON, Canada) mounting medium. Specimens were analyzed using a spinning disc confocal microscope with a 20X objective and the appropriate laser excitation and emission filters (WaveFx from Quorum Technologies, Guelph, Canada).

### 2.11.1 Antibodies and Fluorescent Stains

Primary rabbit anti-Cldn14 antibody was from Invitrogen (Carlsbad, CA, USA; Catalog # 36-4200). The Fluorescein labeled *Lotus Tetragonolobus* Lectin was from Vector Laboratories Inc., Burlington, ON, Canada (Catalog # FL-1321). Mouse anti-

NKCC2 (Sodium- potassium- 2 chloride co-transporter T4) was from the Developmental Studies Hybridoma Bank (Iowa city, IA USA). The rabbit anti-NCC (Sodium chloride co-transporter) was from StressMarq Biosciences Inc. (Victoria, BC Canada) (Catalog # SPC-402D) and mouse anti-calbindin<sub>28K</sub> was from Abcam, (Cambridge, MA, USA) (Catalog # ab82812). Secondary antibodies were: Cy 3-conjugated AffiniPure Donkey Anti-Rabbit (Jackson ImmunoResearch Laboratories, West Grove, PA, USA), DyLight 488-conjugated AffiniPure Donkey Anti-Mouse (Jackson ImmunoResearch Laboratories, West Grove, PA, USA) and DyLight 488-conjugated AffiniPure Donkey Anti- Rabbit (Jackson ImmunoResearch Laboratories, West Grove, PA, USA) were used for immunofluorescence.

### **2.11.2 Validation of antibodies**

Specificity of the Cldn14 antibody (Invitrogen, Carlsbad, CA, USA; Catalog # 36-4200) was confirmed by blotting against overexpressed mouse claudin 14 containing a c-terminal myc tag (OriGene Technologies, Inc., Rockville, MD, USA). The transfection-ready DNA was transiently transfected in HEK293 cells (American Type Culture Collection, Manassas, VA, USA) and grown till confluent. Once 100% confluent, cell lysate was collected after lysing the cells with lysis buffer (20mM Tris pH7.4, 135mM NaCl, 5mM EDTA, 0.1% Triton X100, 0.5% NP-40 and Phosphatase Inhibitor cocktail1: 100). The subsequent cell lysate obtained was loaded on a 12% acrylamide (BioRad, Mississauga, ON, Canada) gel, blotted and then incubated with mouse primary anti-myc (9B11) monoclonal antibody (Cell Signaling Technology Inc., Danvers, MA, USA 1:1000) overnight at 4°C, followed by incubation with a

secondary horseradish peroxidase coupled secondary antibody (SantaCruz CA, USA, 1:5000). Proteins were detected with Western Lightning™ Plus ECL reagents (PerkinElmer Inc., Boston, MA, USA) and visualized using a Carestream *in-vivo* FXPro imaging system (Carestream Health Canada, Vaughan, ON, Canada).

## **2.12 Statistical Analysis**

Data are expressed as mean  $\pm$  SEM. Statistical comparisons were made by one-way ANOVA with a Bonferroni correction for multiple comparisons in experiments with 3 groups. In experiments with only 2 groups statistical comparisons were made with a Mann-Whitney test. A  $p < 0.05$  was considered statistically significant. All analyses were performed using Graphpad Prism software (GraphPad Software Inc., San Diego, CA, USA).

## **CHAPTER 3**

### **RESULTS**

### 3.1 Expression of claudins in kidney

To determine which claudins are expressed in the kidney, polymerase chain reaction (PCR) was carried out with primers specific for each claudin (**Table 2.1**). cDNA from whole murine kidney was used as the template. In the whole kidney, all the claudins except Cldn17 were found to be present (**Figure 3.1**). As a positive control for the PCR reaction, genomic DNA (gDNA) from murine whole kidney was used (this was possible as the PCR primers were designed against a single exon). All the reactions showed a single band of the appropriate molecular size for each claudin (**Figure 3.1**). As a negative control a template generated by performing the reverse transcription reaction in the absence of reverse transcriptase was used. No band was observed for any reaction when this template was used. As further controls, the expression of  $\beta$ -actin, TRPV5, NaPi2a, JAM1, occludin and tricellulin were also determined. Appropriate sized bands were obtained for each of these genes.

PCR was also carried out on cDNA obtained from microdissected proximal tubules to ascertain the expression of claudins in this nephron segment. Claudin (Cldn)- 1, -2, -3, -8, -10a, -10b, -12, -15 and -16 were found to be present (**Figure 3.2**). gDNA from murine whole kidney was used as the positive control for all reactions. All the bands obtained for gDNA were of the right molecular weight. The same negative control was used, noRT. No band was obtained for any of these reactions. GAPDH was used as a positive control for cDNA integrity and the right sized band was obtained. As a positive control for isolation of proximal tubules NaPi2a was used. The exact molecular weight band was obtained in the lane for cDNA. As a control to assess

whether cDNA was contaminated with distal convoluted tubule, TRPV5 was employed. No band was observed in the lane for cDNA. Expression of other tight junction molecules including: occludin, JAM1 and tricellulin was determined to confirm the presence of tight junctions. A correct size band was obtained for each of these genes (**Figure 3.2**).

**Figure 3.1 Claudin expression in whole kidney**

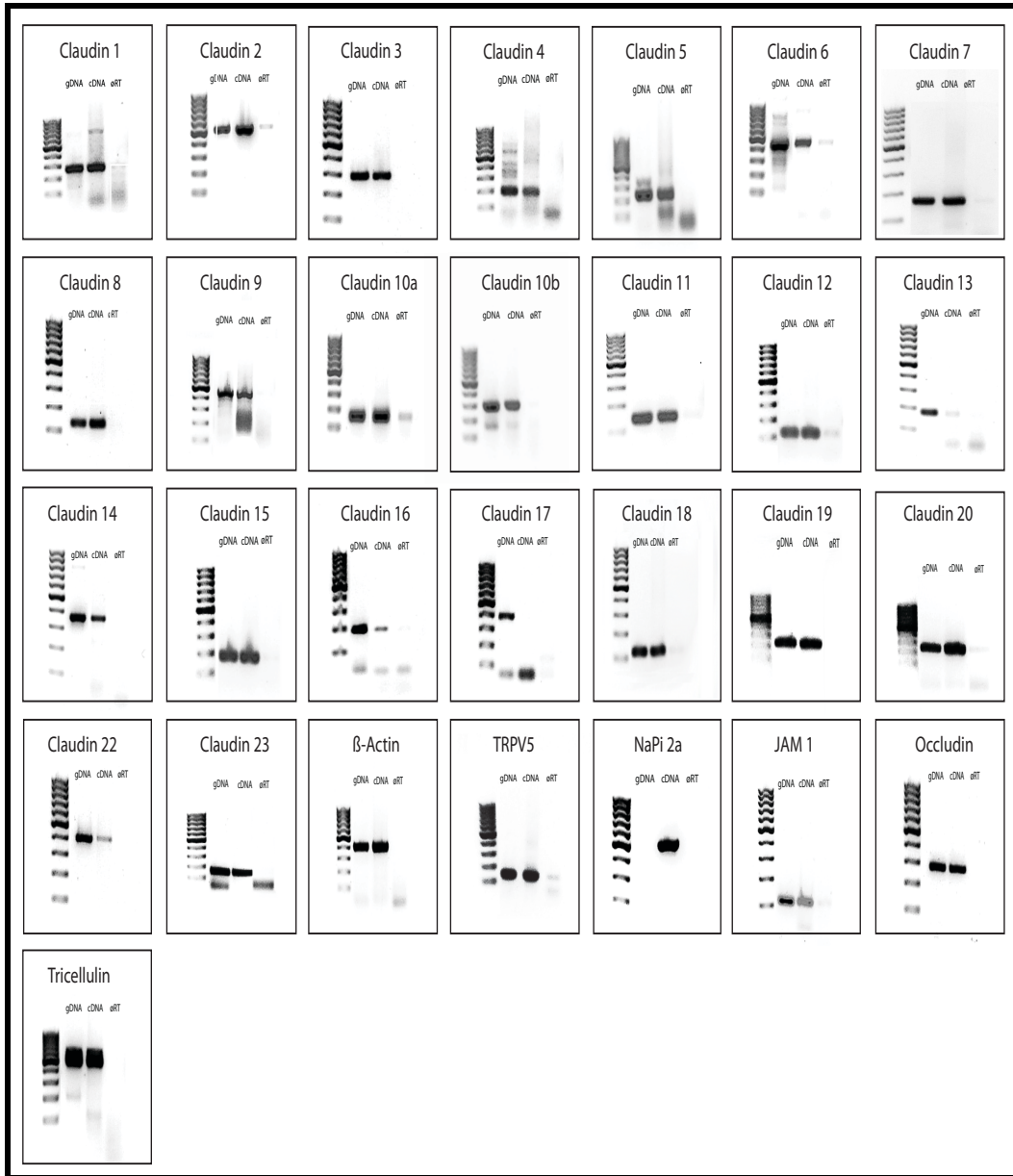


**Figure 3.1:** Expression of claudins in whole kidney by polymerase chain reaction (PCR) on genomic DNA (gDNA), complementary DNA (cDNA) and negative control (noRT). Lane 1- 100bp DNA ladder.

**Figure 3.2. Claudin expression in microdissected proximal tubules**

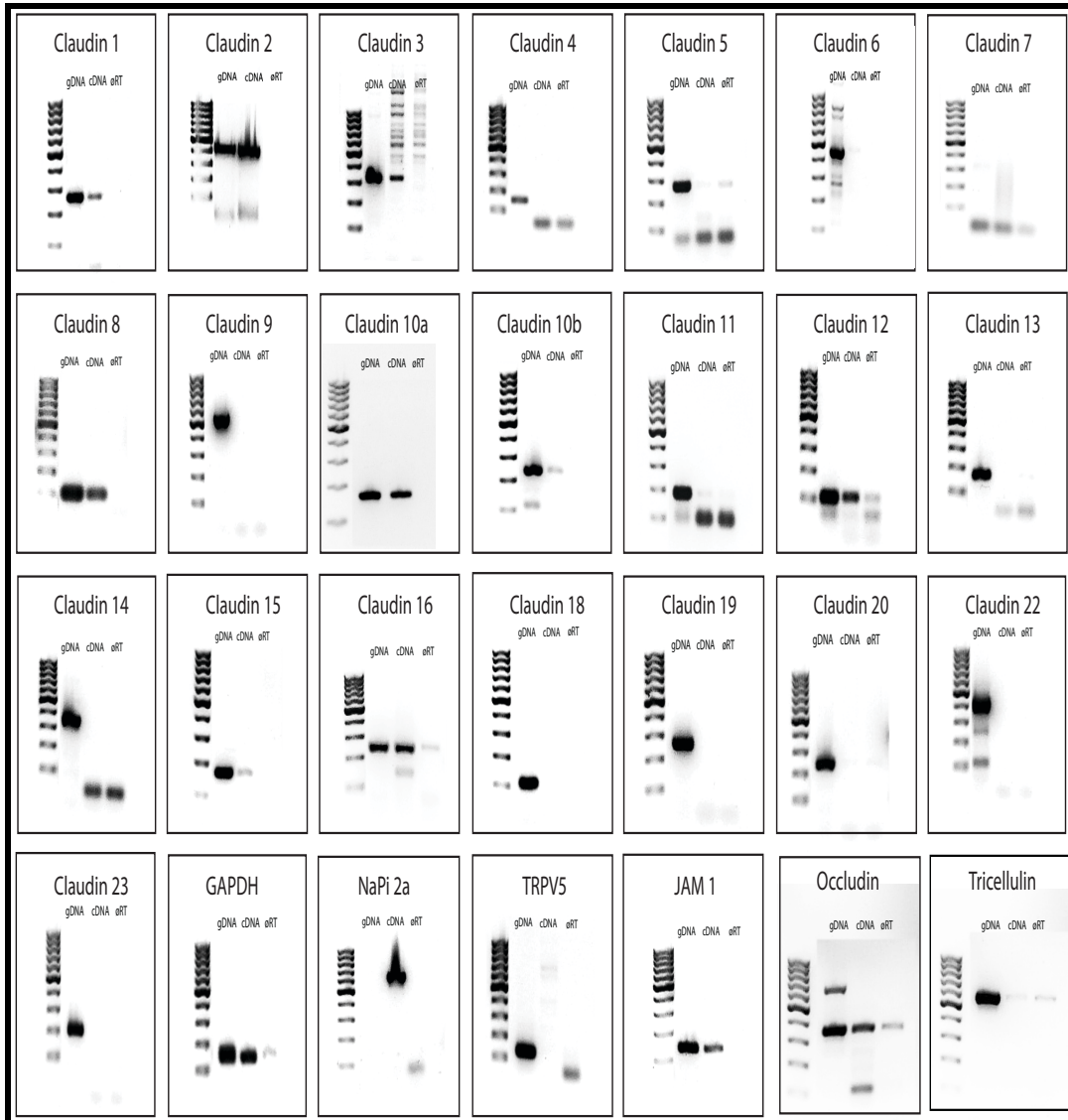


**Figure 3.2:** Expression of claudins in microdissected proximal tubules by polymerase chain reaction (PCR) on genomic DNA (gDNA), complementary DNA (cDNA) and negative control (noRT). Lane 1-100bp DNA ladder.

## 3.2 Ca<sup>2+</sup> diet experiment

### 3.2.1 Blood and Urine data

FVB/N mice were placed on a low (0.01%), normal (0.6%), or high (2%) Ca<sup>2+</sup> diet for either 10 or 21 days, respectively. All animals weighed approximately the same at the end of the experimental period. No difference in the amount of water consumed or urine produced was observed in either experiment. Mice on the low Ca<sup>2+</sup> diet for 10 days showed decreased food intake (**Table 3.1A&B**). The concentration of ionized Ca<sup>2+</sup> in blood was not different between groups (**Figure 3.3A**). Mice on the high Ca<sup>2+</sup> diet showed a slight increase in blood pH at the end of 10 days, however this effect was not observed after 21 days. There was no difference in P<sub>O2</sub>, P<sub>CO2</sub>, HCO<sub>3</sub><sup>-</sup>, Hct and Hb (**Table 3.2A&B**). No statistically significant difference was observed in serum electrolyte concentration or urinary electrolyte excretion (**Table 3.3A&B and 3.4A&B**). The urinary Ca<sup>2+</sup> /creatinine ratio increased proportionally to the amount of Ca<sup>2+</sup> in the diet (**Figure 3.3B and Table 3.5A&B**). The concentration of 1,25-dihydroxyvitamin D<sub>3</sub> (1,25(OH)<sub>2</sub>D<sub>3</sub>) in serum was significantly increased in mice maintained on a low Ca<sup>2+</sup> diet (**Figure 3.3C**). The serum parathyroid hormone (PTH) concentration was significantly reduced in mice on high dietary Ca<sup>2+</sup> for 10 days (**Figure 3.3D**).

**Table 3.1A: Calcium diet experiment (10 days): *Metabolic cage data***

	Weight (g)	H <sub>2</sub> O Drunk (ml/24h)	H <sub>2</sub> O Drunk (ml·g <sup>-1</sup> ·24 h <sup>-1</sup> )	Chow Eaten (g/24h)	Chow Eaten (g·g <sup>-1</sup> ·24 h <sup>-1</sup> )	Urine Volume (ml/24h)	Urine Volume (ml·g <sup>-1</sup> ·24 h <sup>-1</sup> )
<b>Low Ca<sup>2+</sup> diet</b>	24.99 ± 0.90	5.26 ± 1.31	0.19 ± 0.05	3.35 ± 0.20*	0.13 ± 0.01*	0.63 ± 0.14	0.02 ± 0.01
<b>Control diet</b>	24.23 ± 1.09	5.37 ± 0.72	0.22 ± 0.03	3.81 ± 0.16	0.15 ± 0.01	0.90 ± 0.26	0.04 ± 0.01
<b>High Ca<sup>2+</sup> diet</b>	25.94 ± 0.83	4.04 ± 0.33	0.15 ± 0.02	3.80 ± 0.25	0.14 ± 0.01	0.70 ± 0.07	0.03 ± 0.00

Values are mean ± SE. *n* = 14-16 in each group. \**p* < 0.05 when compared with control

**Table 3.1B: Calcium diet experiment (21 days): *Metabolic cage data***

	Weight (g)	H <sub>2</sub> O Drunk (ml/24h)	H <sub>2</sub> O Drunk (ml·g <sup>-1</sup> ·24 h <sup>-1</sup> )	Chow Eaten (g/24h)	Chow Eaten (g·g <sup>-1</sup> ·24 h <sup>-1</sup> )	Urine Volume (ml/24h)	Urine Volume (ml·g <sup>-1</sup> ·24 h <sup>-1</sup> )
<b>Low Ca<sup>2+</sup> diet</b>	24.34 ± 0.96	1.61 ± 2.19	0.07 ± 2.19	4.43 ± 0.16	0.02 ± 0.01	0.38 ± 0.06	0.02 ± 0.003
<b>Control diet</b>	24.99 ± 1.47	3.77 ± 0.44	0.16 ± 0.03	4.30 ± 0.20	0.005 ± 0.01	0.67 ± 0.14	0.03 ± 0.01
<b>High Ca<sup>2+</sup> diet</b>	25.19 ± 1.24	5.90 ± 0.99	0.23 ± 0.03	4.59 ± 0.21	0.02 ± 0.01	0.89 ± 0.25	0.03 ± 0.01

Values are mean ± SE. *n* = 8 in each group, values are not statistically different between groups.

**Figure 3.3: Calcium diet experiment (10 and 21 days)- Blood and urinary data**

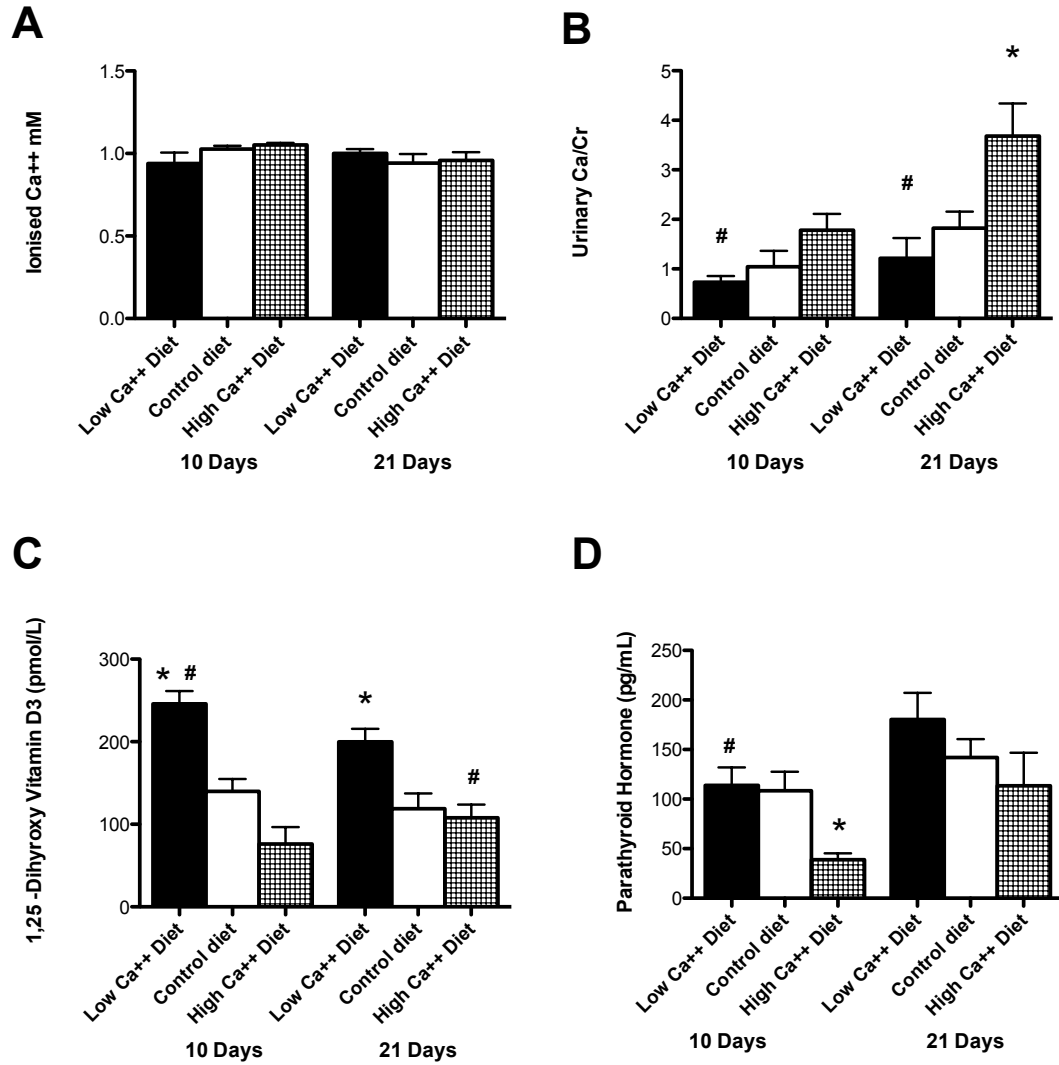


**Figure 3.3:** Plots of Serum Ca<sup>2+</sup> concentration (mM) (A), urinary calcium/creatinine (B), plasma 1,25-Dihydroxy vitamin D<sub>3</sub> concentration (pmol/L) (C) and plasma parathyroid hormone concentration (PTH) (pg/mL) (D) from WT mice on low Ca<sup>2+</sup> diet, control diet and high Ca<sup>2+</sup> diet for a period of 10 days and 21 days respectively. *n*= 6-8 in each group. \**p* <0.05 in comparison to control group and #*p* <0.05 in comparison to high Ca<sup>2+</sup> diet.

**Table 3.2A: Calcium diet experiment (10 days): Blood-gas analysis**

	pH	P <sub>O2</sub> (mm Hg)	P <sub>CO2</sub> (mm Hg)	HCO <sub>3</sub> <sup>-</sup> (mM)	Hct (%)	Hb (g/l)
<b>Low Ca<sup>2+</sup> diet</b>	7.32 ± 0.02	32.67 ± 0.67	36.90 ± 1.97	18.83 ± 0.94	0.38 ± 0.01	129.33 ± 2.03
<b>Control diet</b>	7.33 ± 0.01	30.25 ± 2.43	35.25 ± 2.17	18.53 ± 1.29	0.38 ± 0.01	130.00 ± 4.20
<b>High Ca<sup>2+</sup> diet</b>	7.40 ± 0.01* <sup>#</sup>	32.00 ± 0.58	33.83 ± 1.69	20.73 ± 0.34	0.40 ± 0.0033	135.00 ± 1.00

Values are mean ± SE. *n* = 3-4 in each group. \**p* < 0.05 when compared with control. #*p* < 0.05 when compared with low Ca<sup>2+</sup> diet group.

**Table 3.2B: Calcium diet experiment (21 days): Blood-gas analysis**

	pH	P <sub>O2</sub> (mm Hg)	P <sub>CO2</sub> (mm Hg)	HCO <sub>3</sub> <sup>-</sup> (mM)	Hct (%)	Hb (g/l)
<b>Low Ca<sup>2+</sup> diet</b>	7.32 ± 0.01	26.57 ± 1.41	40.75 ± 1.12	21.16 ± 0.57	0.38 ± 0.01	130.33 ± 2.25
<b>Control diet</b>	7.29 ± 0.03	25.67 ± 0.70	40.23 ± 3.10	19.36 ± 1.05	0.38 ± 0.01	127.67 ± 3.13
<b>High Ca<sup>2+</sup> diet</b>	7.33 ± 0.03	30.43 ± 1.92	36.30 ± 2.25	19.47 ± 1.83	0.38 ± 0.01	127.86 ± 3.97

Values are mean ± SE. *n* = 8 in each group. \**p* < 0.05 when compared with control.

**Table 3.3A: Calcium diet experiment (10 days): Serum electrolytes**

	<b>Na<sup>+</sup> (mM)</b>	<b>K<sup>+</sup> (mM)</b>	<b>Ca<sup>2+</sup> (mM)</b>	<b>Glucose (mM)</b>
<b>Low Ca<sup>2+</sup> diet</b>	145.00 ± 0.00	4.47 ± 0.15	1.07 ± 0.02	11.43 ± 0.58
<b>Control diet</b>	143.00 ± 0.71	4.53 ± 0.15	1.03 ± 0.03	12.23 ± 0.64
<b>High Ca<sup>2+</sup> diet</b>	141.67 ± 0.33	4.53 ± 0.19	1.06 ± 0.02	14.60 ± 0.62

Values are mean ± SE. *n* = 5-6 in each group, values are not statistically different between groups.

**Table 3.3B: Calcium diet experiment (21 days): Serum electrolytes**

	<b>Na<sup>+</sup> (mM)</b>	<b>K<sup>+</sup> (mM)</b>	<b>Ca<sup>2+</sup> (mM)</b>	<b>Glucose (mM)</b>
<b>Low Ca<sup>2+</sup> diet</b>	142.17 ± 0.93	4.93 ± 0.20	1.00 ± 0.02	12.72 ± 0.55
<b>Control diet</b>	142.17 ± 1.25	5.28 ± 0.42	0.94 ± 0.05	12.67 ± 1.02
<b>High Ca<sup>2+</sup> diet</b>	142.14 ± 1.38	5.90 ± 0.52	0.96 ± 0.05	11.41 ± 1.13

Values are mean ± SE. *n* = 6-7 in each group, values are not statistically different between groups

**Table 3.4A: Calcium diet experiment (10 days): *Urine electrolytes***

	Na <sup>+</sup> ( $\mu\text{mol}/24$ h)	Na <sup>+</sup> ( $\mu\text{mol}\cdot\text{g}^{-1}\cdot 24$ $\text{h}^{-1}$ )	K <sup>+</sup> ( $\mu\text{mol}/$ 24 h)	K <sup>+</sup> ( $\mu\text{mol}\cdot\text{g}^{-1}$ $\cdot 24$ h <sup>-1</sup> )	Cl <sup>-</sup> ( $\mu\text{mol}/$ 24 h)	Cl <sup>-</sup> ( $\mu\text{mol}\cdot\text{g}^{-1}$ $\cdot 24$ h <sup>-1</sup> )	PO <sub>4</sub> <sup>2-</sup> ( $\mu\text{mol}/24$ h)	PO <sub>4</sub> <sup>2-</sup> ( $\mu\text{mol}\cdot\text{g}^{-1}$ $\cdot 24$ h <sup>-1</sup> )	SO <sub>4</sub> <sup>2-</sup> ( $\mu\text{mol}/24$ h)	SO <sub>4</sub> <sup>2-</sup> ( $\mu\text{mol}\cdot\text{g}^{-1}\cdot 24$ h <sup>-1</sup> )
<b>Low Ca<sup>2+</sup> diet</b>	61.21 ± 15.83	2.40 ± 0.71	192.50 ± 39.30	7.50 ± 1.78	66.07 ± 15.87	2.58 ± 0.70	45.74 ± 10.46	1.79 ± 0.47	19.39 ± 3.85	0.76 ± 0.18
	73.94 ± 20.90	2.81 ± 0.76	233.55 ± 61.54	8.90 ± 2.23	67.75 ± 14.58	2.59 ± 0.52	20.91 ± 5.41	0.80 ± 0.20	22.50 ± 5.98	0.86 ± 0.22
<b>High Ca<sup>2+</sup> diet</b>	112.82 ± 10.87 <sup>#</sup>	4.13 ± 0.30	311.33 ± 29.04	11.50 ± 1.34	108.51 ± 12.28	3.97 ± 0.39	21.34 ± 1.42	0.79 ± 0.09	32.80 ± 2.81	1.21 ± 0.12

Values are mean ± SE.  $n=7$  in each group. <sup>#</sup> $p < 0.05$  when compared with low Ca<sup>2+</sup> diet group.

**Table 3.4B: Calcium diet experiment (21 days): *Urine electrolytes***

	Na <sup>+</sup> ( $\mu\text{mol}/24$ h)	Na <sup>+</sup> ( $\mu\text{mol}\cdot\text{g}^{-1}$ $\cdot 24$ h <sup>-1</sup> )	K <sup>+</sup> ( $\mu\text{mol}/$ 24 h)	K <sup>+</sup> ( $\mu\text{mol}\cdot\text{g}^{-1}$ $\cdot 24$ h <sup>-1</sup> )	Cl <sup>-</sup> ( $\mu\text{mol}/$ 24 h)	Cl <sup>-</sup> ( $\mu\text{mol}\cdot\text{g}^{-1}$ $\cdot 24$ h <sup>-1</sup> )	PO <sub>4</sub> <sup>2-</sup> ( $\mu\text{mol}/24$ h)	PO <sub>4</sub> <sup>2-</sup> ( $\mu\text{mol}\cdot\text{g}^{-1}\cdot 24$ h <sup>-1</sup> )
<b>Low Ca<sup>2+</sup> diet</b>	80.32 ± 9.12	3.37 ± 0.46	224.98 ± 28.33*	9.52 ± 1.46	86.70 ± 8.54	3.63 ± 0.42	55.23 ± 6.14*	2.32 ± 0.31*
	102.03 ± 6.72	4.23 ± 0.45	328.41 ± 32.06	13.75 ± 1.88	106.77 ± 9.12	4.48 ± 0.59	33.99 ± 2.65	1.43 ± 0.19
<b>High Ca<sup>2+</sup> diet</b>	89.06 ± 17.06	3.53 ± 0.77	288.78 ± 53.52	11.47 ± 2.45	96.46 ± 19.54	3.89 ± 0.95	11.85 ± 3.27* <sup>#</sup>	0.45 ± 0.11* <sup>#</sup>

Values are mean ± SE.  $n = 7-8$  in each group. \* $p < 0.05$  when compared with control. <sup>#</sup> $p < 0.05$  when compared with low Ca<sup>2+</sup> diet group.

**Table 3.5A: Calcium diet experiment (10 days): Urine analysis**

	pH	Ca <sup>2+</sup> ( $\mu\text{mol}/24\text{ h}$ )	Ca <sup>2+</sup> ( $\mu\text{mol}\cdot\text{g}^{-1}\cdot$ $24\text{ h}^{-1}$ )	Creatinine ( $\mu\text{mol}/24$ )	Creatinine ( $\mu\text{mol}\cdot\text{g}^{-1}\cdot$ $24\text{h}^{-1}$ )	Ca <sup>2+</sup> / Creatinine Ratio
<b>Low Ca<sup>2+</sup> diet</b>	5.23 $\pm$ 0.09*	2.40 $\pm$ 0.74	0.09 $\pm$ 0.03	3.78 $\pm$ 1.14	0.14 $\pm$ 0.04	0.73 $\pm$ 0.15
<b>Control diet</b>	6.13 $\pm$ 0.13	4.83 $\pm$ 2.07	0.14 $\pm$ 0.08	6.66 $\pm$ 4.59	0.20 $\pm$ 0.17	1.04 $\pm$ 0.37
<b>High Ca<sup>2+</sup> diet</b>	6.50 $\pm$ 0.19 <sup>#</sup>	5.71 $\pm$ 1.20 <sup>#</sup>	0.17 $\pm$ 0.05 <sup>#</sup>	3.35 $\pm$ 0.42*	0.10 $\pm$ 0.02	1.78 $\pm$ 0.38 <sup>#</sup>

Values are mean  $\pm$  SE.  $n = 10-11$  in each group. \* $p < 0.05$  when compared with control and <sup>#</sup> $p < 0.05$  when compared with low Ca<sup>2+</sup> diet group.

**Table 3.5B: Calcium diet experiment (21 days): Urine analysis**

	pH	Ca <sup>2+</sup> ( $\mu\text{mol}/24\text{ h}$ )	Ca <sup>2+</sup> ( $\mu\text{mol}\cdot\text{g}^{-1}\cdot$ $24\text{ h}^{-1}$ )	Creatinine ( $\mu\text{mol}/24$ )	Creatinine ( $\mu\text{mol}\cdot\text{g}^{-1}\cdot$ $24\text{h}^{-1}$ )	Ca <sup>2+</sup> / Creatinine Ratio
<b>Low Ca<sup>2+</sup> diet</b>	5.00 $\pm$ 0.00*	3.38 $\pm$ 0.64*	0.06 $\pm$ 0.02*	4.37 $\pm$ 0.52	0.07 $\pm$ 0.02	0.80 $\pm$ 0.12*
<b>Control diet</b>	5.75 $\pm$ 0.09	5.71 $\pm$ 0.83	0.16 $\pm$ 0.04	3.99 $\pm$ 0.55	0.12 $\pm$ 0.03	1.53 $\pm$ 0.25
<b>High Ca<sup>2+</sup> diet</b>	6.81 $\pm$ 0.13* <sup>#</sup>	14.94 $\pm$ 3.27 <sup>#</sup>	0.67 $\pm$ 0.26 <sup>#</sup>	3.75 $\pm$ 0.69	0.16 $\pm$ 0.06	4.19 $\pm$ 0.59* <sup>#</sup>

Values are mean  $\pm$  SE.  $n = 8$  in each group. \* $p < 0.05$  when compared with control. <sup>#</sup> $p < 0.05$  when compared with low Ca<sup>2+</sup> diet group.

### 3.2.2 RNA expression of claudins in whole kidney

The renal expression of claudin-2, -10a, -12, -15, -16 and -19 was not altered by ingestion of a diet that is either low or high in  $\text{Ca}^{2+}$  content (**Figure 3.4- A-G**). All samples were normalized to the expression of 18S, as we were unable to detect a difference in the expression level of 18S between different diets. Mice maintained on a high  $\text{Ca}^{2+}$  diet had a >2-fold increase in the renal expression of Cldn14 after 10 days and >3-fold increase after 21 days. There was no alteration in renal Cldn14 expression observed in mice on a low  $\text{Ca}^{2+}$  diet (**Figure 3.4-D**). No change was observed in the expression of claudin- 1, -3 and -8 on low  $\text{Ca}^{2+}$  or high  $\text{Ca}^{2+}$  diet after 10 days (**Figure 3.5- A-C**). We did not measure the expression of these claudins after 21 days on diets with different amounts of  $\text{Ca}^{2+}$  in it. Consistent with the systemic vitamin  $\text{D}_3$  levels, renal expression of  $1\alpha$ -hydroxylase ( $1\alpha$ -OHase), the enzyme responsible for the generation of active  $1,25(\text{OH})_2\text{D}_3$  was significantly increased in mice maintained on a low  $\text{Ca}^{2+}$  diet (**Table 3.6**). Conversely, expression of vitamin D-24-hydroxylase (24-OHase) the enzyme that catabolizes active  $1,25(\text{OH})_2\text{D}_3$  into its inactive form was significantly increased in animals maintained on a high  $\text{Ca}^{2+}$  diet (**Table 3.6**).

**Figure 3.4: Calcium diet experiment (10 and 21 days): RNA expression of claudins in whole kidney**

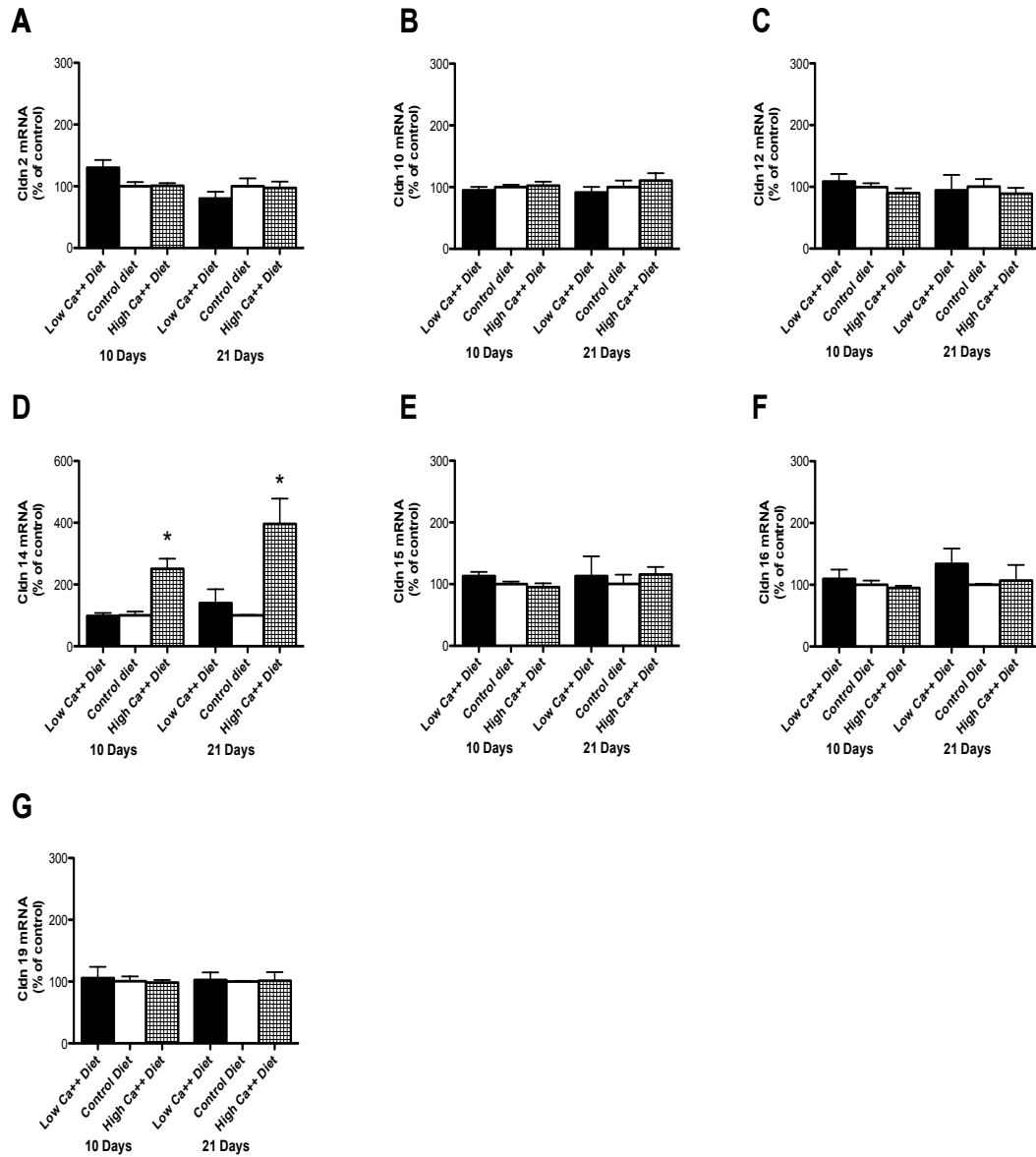


**Figure 3.4:** qPCR analysis of Cldn 2 (A), Cldn 10a (B), Cldn 12 (C), Cldn 14 (D), Cldn 15 (E), Cldn 16 (F), Cldn 19 (G) expression in whole kidney of mice on diets containing different amounts of Ca<sup>2+</sup>. The results are expressed as a percentage of control group and are normalized to the expression of 18s. *n* = 8-14 in each group. \**p* < 0.05 in comparison to control group.

**Figure 3.5: Calcium diet experiment (10 days): RNA expression of claudins in whole kidney**

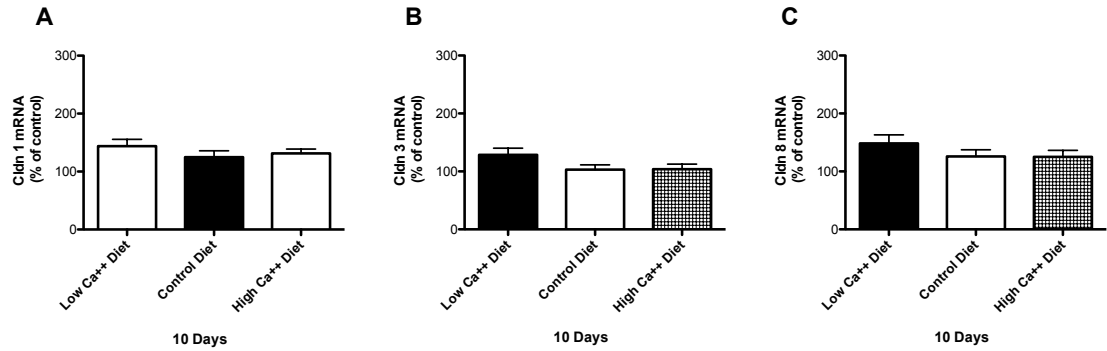


**Figure 3.5:** qPCR analysis of Cldn1 (A), Cldn3 (B) and Cldn8 (C) expression in whole kidney. The results are expressed as a percentage of control group and are normalized to the expression of 18s.  $n=8$  in each group. Values are not statistically different between groups.

**Table 3.6: Calcium diet experiment (10 and 21 days): RNA expression of 1 $\alpha$ -OHase and 24-OHase**

	1 $\alpha$ Hydroxylase (%)		24 $\alpha$ Hydroxylase (%)	
	10 days	21 days	10 days	21 days
<b>Low Ca<sup>2+</sup> diet</b>	231.93 $\pm$ 40.49*	340.61 $\pm$ 79.27*	80.86 $\pm$ 23.66	139.52 $\pm$ 45.23
<b>Control diet</b>	100.27 $\pm$ 13.95	100 $\pm$ 0.65	100.02 $\pm$ 13.63	99.99 $\pm$ 2.65
<b>High Ca<sup>2+</sup> diet</b>	91.60 $\pm$ 11.98 <sup>#</sup>	92.09 $\pm$ 18.51 <sup>#</sup>	285.07 $\pm$ 60.59* <sup>#</sup>	396.42 $\pm$ 81.62* <sup>#</sup>

Values are mean  $\pm$  SE, and expressed as a percentage of the control diet expression.  $n = 7-8$  in each group. \* $p < 0.05$  when compared with control. <sup>#</sup> $p < 0.05$  when compared with low Ca<sup>2+</sup> diet group.

### 3.3 Vitamin D experiment

To determine the potential role of  $1,25(\text{OH})_2\text{D}_3$  on the expression of *Cldn14*, animals received daily intraperitoneal injections of  $1,25(\text{OH})_2\text{D}_3$  or vehicle for 5 days.  $1,25(\text{OH})_2\text{D}_3$  promotes intestinal hyperabsorption and renal reabsorption of  $\text{Ca}^{2+}$ .

Handling of the animals (placing the animals in metabolic cages, injecting the animal with  $1,25(\text{OH})_2\text{D}_3$ , collecting urine, blood and tissue samples) and real-time PCR for claudin -2, -12, -14, -15, -16 and -19 for this experiment was done by Dr. Henrik Dimke.

#### 3.3.1 Blood and Urinary data

Body weight, water consumed and urine output of animals in control or treatment group were not significantly different. Mice in the treatment group eat less food than their counterparts in the control group (**Table 3.7**). No difference in  $\text{P}_{\text{O}_2}$ ,  $\text{HCO}_3^-$  and Hct was observed.  $\text{P}_{\text{CO}_2}$  of animals in the treated group was found to be higher (**Table 3.8**). Animals injected with  $1,25(\text{OH})_2\text{D}_3$  developed significantly increased levels of ionized  $\text{Ca}^{2+}$  in their blood (**Figure 3.6A and Table 3.9**). The urinary  $\text{Ca}^{2+}$  /Creatinine ratio was also elevated in these animals, but it did not reach statistical significance (**Figure 3.6B and Table 3.10**). No difference in urine electrolyte excretion was detected (**Table 3.11**). Serum  $1,25(\text{OH})_2\text{D}_3$  levels were increased significantly while PTH was undetectable in the mice administered  $1,25(\text{OH})_2\text{D}_3$  (**Figure 3.6C-D**).

**Table 3.7: Vitamin D experiment: *Metabolic cage data***

	Weight (g)	H <sub>2</sub> O Drunk (ml/24h)	H <sub>2</sub> O Drunk, (ml·g <sup>-1</sup> · 24 h <sup>-1</sup> )	Chow Eaten (g/24h)	Chow Eaten (g·g <sup>-1</sup> ·24 h <sup>-1</sup> )	Urine Volume (ml/24h)	Urine Volume (μl·g <sup>-1</sup> · 24 h <sup>-1</sup> )
<b>Control</b>	23.07 ± 1.00	3.91 ± 0.23	0.17 ± 0.01	2.73 ± 0.23	0.12 ± 0.01	0.67 ± 0.13	0.03 ± 0.01
<b>1,25- dihydroxy vitamin D<sub>3</sub></b>	22.98 ± 1.07	3.73 ± 0.25	0.16 ± 0.01	1.48 ± 0.39*	0.07 ± 0.02*	0.71 ± 0.12	0.03 ± 0.005

Values are mean ± SE. *n* = 8 in each group. \**p* < 0.05 when compared with control

**Table 3.8: Vitamin D experiment: *Blood-gas analysis***

	pH	P <sub>O<sub>2</sub></sub> (mm Hg)	P <sub>CO<sub>2</sub></sub> (mm Hg)	HCO <sub>3</sub> <sup>-</sup> (mM)	Hct (%)
<b>Control</b>	7.38 ± 0.01	30.57 ± 1.48	36.29 ± 0.86	21.44 ± 0.45	0.37 ± 0.001
<b>1,25- dihydroxy vitamin D<sub>3</sub></b>	7.37 ± 0.01	29.13 ± 1.75	40.41 ± 1.41*	23.14 ± 0.86	0.37 ± 0.01

Values are mean ± SE. *n* = 8 in each group. \**p* < 0.05 when compared with control.

**Figure 3.6 Vitamin D experiment: Blood and urinary data**

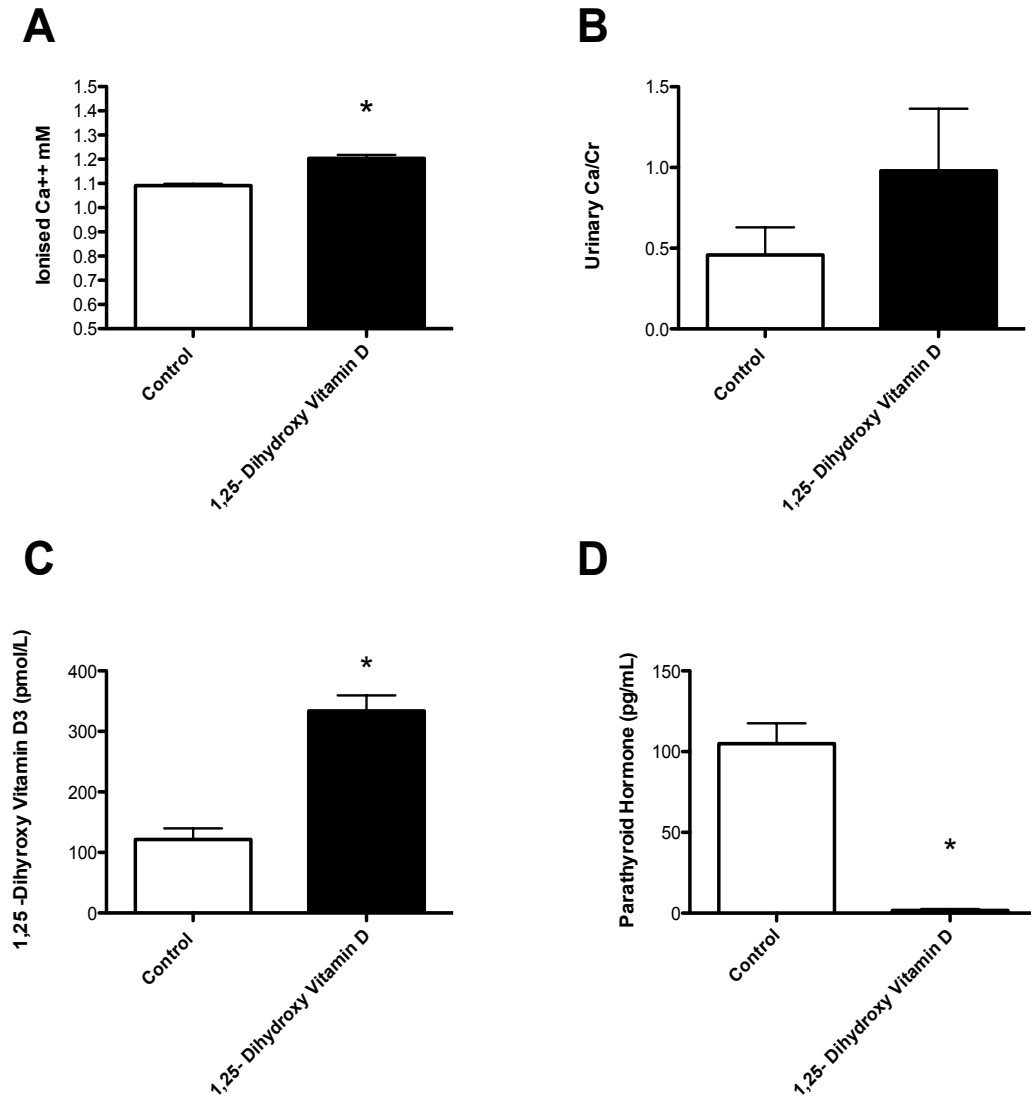


**Figure 3.6:** Plots of Serum  $\text{Ca}^{2+}$  concentration (mM) (A), urinary calcium/creatinine (B), plasma 1,25-Dihydroxy vitamin D3 concentration (pmol/L) (C) and plasma parathyroid hormone concentration (PTH) (pg/mL) (D) from WT mice and mice injected with 1,25-dihydroxy vitamin D for a period of 5 days.  $n=8$  in per group. \* $p < 0.05$  in comparison to control group.

**Table 3.9: Vitamin D experiment: Serum electrolytes**

	Na <sup>+</sup> (mM)	K <sup>+</sup> (mM)	Ca <sup>2+</sup> (mM)
<b>Control</b>	145.71 ± 0.27	4.47 ± 0.10	1.09 ± 0.01
<b>1,25-dihydroxy vitamin D<sub>3</sub></b>	145.00 ± 0.38	4.80 ± 0.19	1.20 ± 0.01*

Values are mean ± SE. *n* = 8 in each group. \**p* < 0.05 when compared with control.

**Table 3.10: Vitamin D experiment: Urine analysis**

	Ca <sup>2+</sup> (mmol/ 24 h)	Ca <sup>2+</sup> (μmol·g <sup>-1</sup> ·24 h <sup>-1</sup> )	Creatinine (mmol /24h)	Creatinine (μmol·g <sup>-1</sup> ·24 h <sup>-1</sup> )	Ca <sup>2+</sup> /Creatinine Ratio
<b>Control</b>	1.41 ± 0.53	0.06 ± 0.02	3.95 ± 0.47	0.17 ± 0.02	0.30 ± 0.08
<b>1,25- dihydroxy vitamin D<sub>3</sub></b>	4.90 ± 2.54*	0.20 ± 0.09	3.89 ± 0.52	0.17 ± 0.02	1.04 ± 0.44

Values are mean ± SE. *n* = 8 in each group. \**p* < 0.05 when compared with control.

**Table 3.11: Vitamin D experiment: Urine electrolytes**

	Na <sup>+</sup> (μmol/ 24 h)	Na <sup>+</sup> (μmol·g <sup>-1</sup> ·24 h <sup>-1</sup> )	K <sup>+</sup> (μmol/ 24 h)	K <sup>+</sup> (μmol·g <sup>-1</sup> ·24 h <sup>-1</sup> )	Cl <sup>-</sup> (μmol/ 24 h)	Cl <sup>-</sup> (μmol·g <sup>-1</sup> ·24 h <sup>-1</sup> )	PO <sub>4</sub> <sup>2-</sup> (μmol/ 24 h)	PO <sub>4</sub> <sup>2-</sup> (μmol·g <sup>-1</sup> ·24 h <sup>-1</sup> )
<b>Control</b>	236.06 ± 31.61	10.38 ± 1.37	434.11 ± 63.51	19.14 ± 2.83	390.99 ± 50.67	17.23 ± 2.30	26.48 ± 3.37	1.16 ± 0.15
<b>1,25- dihydroxy vitamin D<sub>3</sub></b>	235.19 ± 31.01	10.21 ± 0.88	405.87 ± 49.27	17.79 ± 1.71	361.33 ± 40.57	15.86 ± 1.31	25.31 ± 6.11	1.08 ± 0.23

Values are mean ± SE. *n* = 8 in each group, values are not statistically different between groups.

### 3.3.2 RNA expression of claudins in whole kidney

No change in the renal expression of claudin-2, -10a, -12, -15, -16 and -19 was observed in mice injected with  $1,25(\text{OH})_2\text{D}_3$  (**Figure 3.7**). Renal Cldn14 mRNA expression was elevated 10-fold in animals injected with  $1,25(\text{OH})_2\text{D}_3$  (**Figure 3.7D**). Expression of  $1\alpha\text{-OHase}$  was significantly decreased and  $24\text{-OHase}$  expression was increased (**Table 3.12**).

### 3.3.3 Cldn14 protein expression

An increase in the expression of claudin-14 protein was observed by immunostaining on kidney sections of mice injected with  $1,25(\text{OH})_2\text{D}_3$  when compared to kidney sections of control mice (**Figure 3.8**).

**Figure 3.7 Vitamin D experiment: RNA expression of claudins in whole kidney**

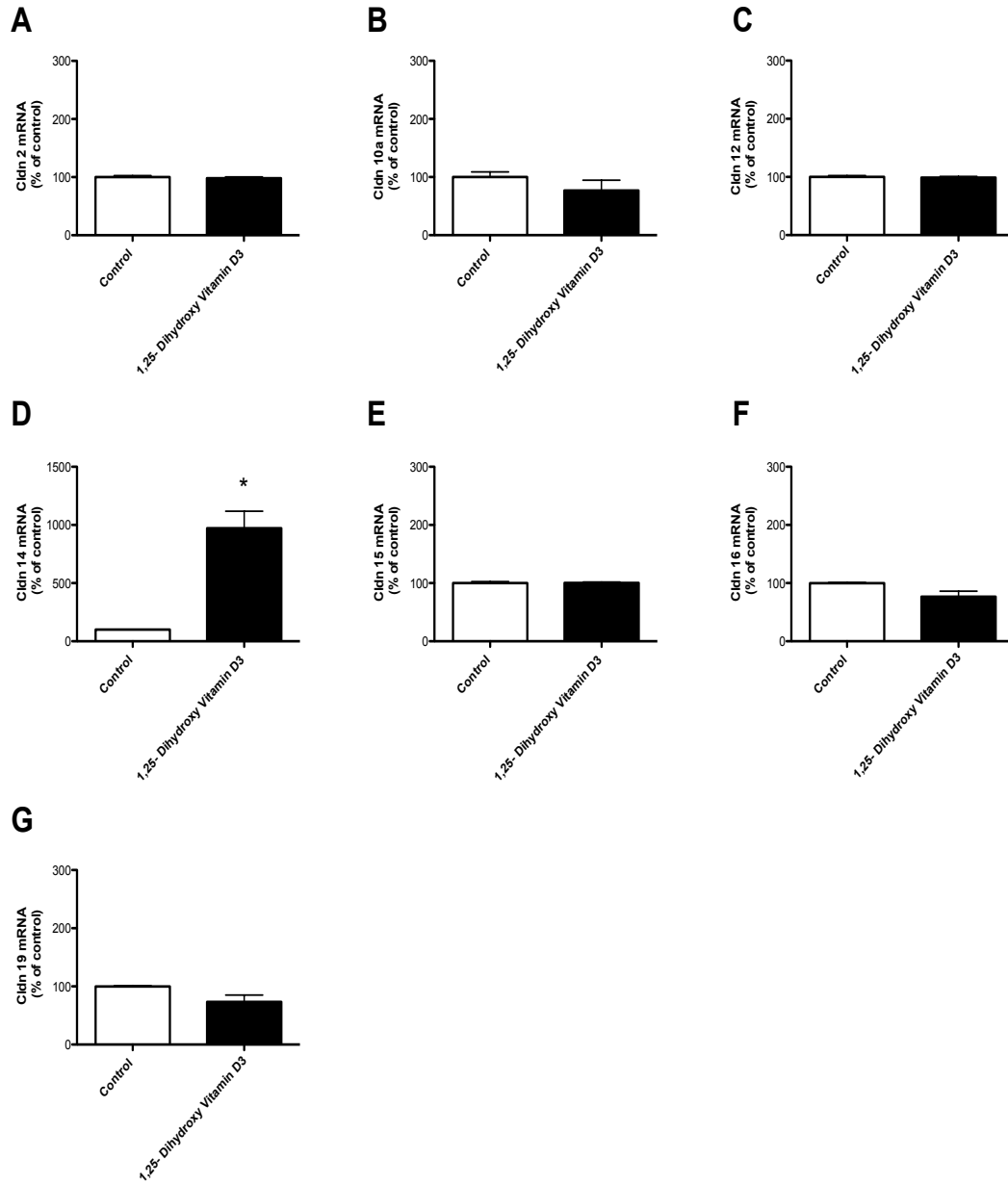


**Figure 3.7:** qPCR analysis of Cldn2 (A), Cldn10a (B), Cldn12 (C), Cldn14 (D), Cldn15 (E), Cldn16 (F), Cldn19 (G) expression in whole kidney of mice injected with vehicle (control) and mice injected with 1,25-dihydroxy vitamin D<sub>3</sub>. The results are expressed as a percentage of control group and are normalized to the expression of 18S.  $n = 8$  in each group. \* $p < 0.05$  in comparison to control group.

**Table 3.12: Vitamin D experiment: RNA expression of 1 $\alpha$ -OHase and 24-OHase**

	1 $\alpha$ Hydroxylase (%)	24 $\alpha$ Hydroxylase (%)
Control	100 $\pm$ 1.43	100 $\pm$ 1.30
1,25-dihydroxy vitamin D <sub>3</sub>	9.17 $\pm$ 1.16*	6170.79 $\pm$ 1173.83*

Values are mean  $\pm$  SE.  $n = 8$  in each group. \* $p < 0.05$  when compared with control.

**Figure 3.8 Vitamin D experiment: Immunostaining for Cldn14**

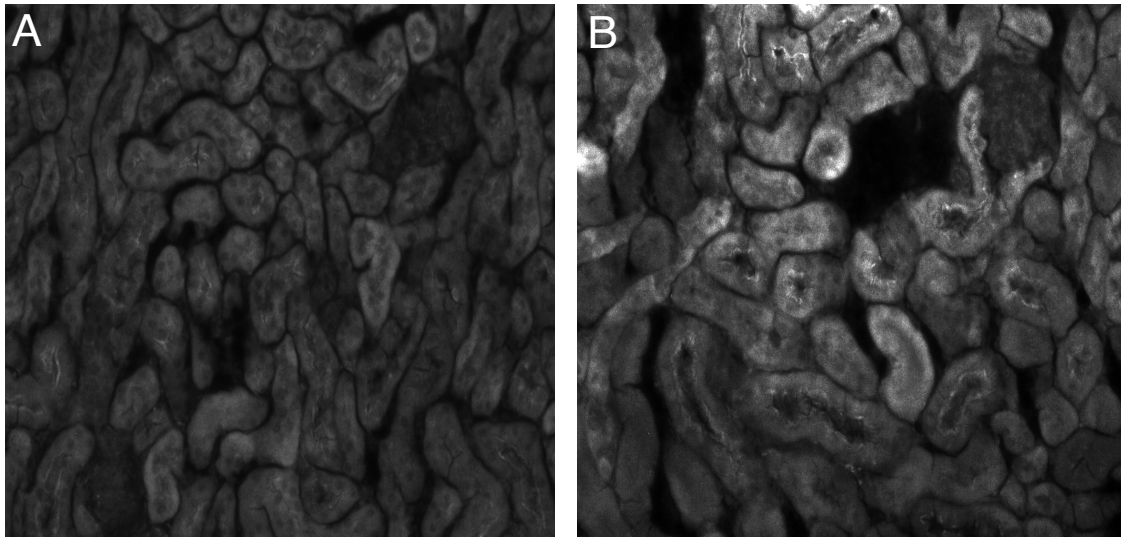


**Figure 3.8:** Low power images of immunostaining for Cldn14 of renal sections of wild type (A) and 1,25-dihydroxy vitamin D<sub>3</sub> injected (B) mice.

### 3.4 Cinacalcet experiment

Renal Cldn14 expression was elevated on a high  $\text{Ca}^{2+}$  diet, a condition suppressing PTH and  $1,25(\text{OH})_2\text{D}_3$ . In contrast, administration of  $1,25(\text{OH})_2\text{D}_3$  increased Cldn14 expression by 10-fold, while a low  $\text{Ca}^{2+}$  diet had no effect on Cldn14 expression, even though it decreased  $1,25(\text{OH})_2\text{D}_3$  levels. Taken together the data suggests that elevated serum  $\text{Ca}^{2+}$  is responsible for stimulating renal Cldn14 expression. To test this hypothesis animals were administered the calcimimetic, Cinacalcet.

Handling of the animals (placing the animals in metabolic cages, treating the animals with cinacalcet, collecting urine, blood and tissue samples) and real-time PCR for claudin -2, -12, -14, -15, -16 and -19 for this experiment was done by Dr. Henrik Dimke.

#### 3.4.1 Blood and Urinary data

Animals given cinacalcet weighed less and eat less than the control group animals (**Table 3.13**). No difference was observed in the pH,  $\text{P}_{\text{CO}_2}$ ,  $\text{P}_{\text{O}_2}$ ,  $\text{HCO}_3^-$  and Hct of these animals (**Table 3.14**). Ionized  $\text{Ca}^{2+}$  was significantly reduced, as expected from CaSR hyperactivation (**Figure 3.9A and Table 3.15**). Consistent with this, animals receiving Cinacalcet developed tetany by the end of the experimental period. The urinary  $\text{Ca}^{2+}$ /Creatinine ratio was significantly elevated in animals treated with Cinacalcet (**Figure 3.9B and Table 3.16**). Serum  $1,25\text{-(OH)}_2\text{-Vit D}_3$  levels remained unaltered, while serum PTH levels were undetectable (**Figure 3.9C-D**).

**Table 3.13: Cinacalcet experiment: *Metabolic cage data***

	Weight (g)	H <sub>2</sub> O Drunk (ml/24h)	H <sub>2</sub> O Drunk (ml·g <sup>-1</sup> ·24 h <sup>-1</sup> )	Chow Eaten (g/24h)	Chow Eaten (g·g <sup>-1</sup> ·24 h <sup>-1</sup> )	Urine Volume (ml/24h)	Urine Volume (μl·g <sup>-1</sup> ·24 h <sup>-1</sup> )
<b>Control</b>	24.77 ± 1.42	5.78 ± 0.69	0.24 ± 0.03	4.13 ± 0.25	0.17 ± 0.02	4.22 ± 0.15	0.05 ± 0.01
<b>Cinacalcet</b>	20.01 ± 1.32*	3.58 ± 0.92	0.19 ± 0.06	1.68 ± 0.16*	0.09 ± 0.01*	3.83 ± 0.41	0.05 ± 0.03

Values are mean ± SE. *n* = 6 in each group. \**p* < 0.05 when compared with control.

**Table 3.14: Cinacalcet experiment: *Blood-gas analysis***

	pH	P <sub>O2</sub> (mm Hg)	P <sub>CO2</sub> (mm Hg)	HCO <sub>3</sub> <sup>-</sup> (mM)	Hct (%)
<b>Control</b>	7.36 ± 0.01	27.80 ± 1.34	41.12 ± 0.60	23.44 ± 0.27	0.39 ± 0.004
<b>Cinacalcet</b>	7.39 ± 0.01	34 ± 2.97	45.87 ± 2.14	27.38 ± 0.8	0.41 ± 0.01

Values are mean ± SE. *n* = 6 in each group, values are not statistically different between groups.

**Table 3.15 Cinacalcet experiment: *Serum electrolytes***

	Na <sup>+</sup> (mM)	K <sup>+</sup> (mM)	Ca <sup>2+</sup> (mM)
<b>Control</b>	146.00 ± 0.63	4.82 ± 0.26	1.08 ± 0.01
<b>Cinacalcet</b>	146.67 ± 0.33	4.90 ± 0.14	0.62 ± 0.02*

Values are mean ± SE. *n* = 6 in each group. \**p* < 0.05 when compared with control.

**Table 3.16 Cinacalcet experiment: *Urine analysis***

	Ca <sup>2+</sup> (μmol/ 24 h)	Ca <sup>2+</sup> (nmol·g <sup>-1</sup> ·24 h <sup>-1</sup> )	Creatinine (μmol/ 24 h)	Creatinine (nmol·g <sup>-1</sup> ·24 h <sup>-1</sup> )	Ca <sup>2+</sup> /Creatinine Ratio
<b>Control</b>	2.03 ± 0.64	0.08 ± 0.03	5.15 ± 0.33	0.21 ± 0.02	0.38 ± 0.11
<b>Cinacalcet</b>	3.24 ± 0.66	0.17 ± 0.04	2.81 ± 0.11	0.14 ± 0.01	1.21 ± 0.26*

Values are mean ± SE. *n* = 6 in each group. \**p* < 0.05 when compared with control

**Figure 3.9** Cinacalcet experiment: *Blood and urinary data*

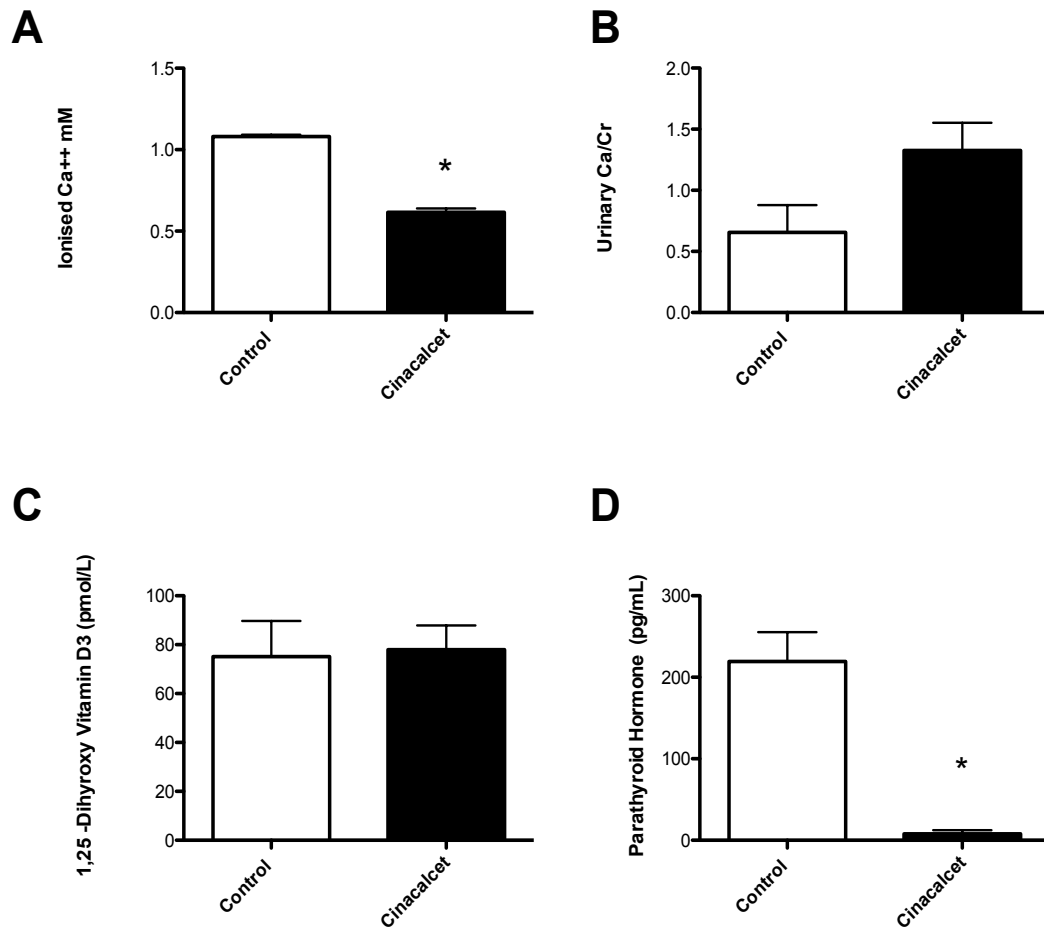


**Figure 3.9:** Plots of Serum Ca<sup>2+</sup> concentration (mM) (A), urinary calcium/creatinine (B), plasma 1,25-Dihydroxy vitamin D<sub>3</sub> concentration (pmol/L) (C) and plasma parathyroid hormone concentration (PTH) (pg/mL) (D) from WT mice on control diet and Cinacalcet treated food for a period of 6 days.  $n=6$  in per group. \* $p < 0.05$  in comparison to control group

### 3.4.2 RNA expression of claudins in whole kidney

Expression of claudin-2, -10a, -12, -15 and -19 remained unchanged in mice treated with cinalcalet (**Figure 3.10**). The expression of Cldn16 increased significantly in the treatment group (**Figure 3.10F**). Renal mRNA expression of Cldn14 was increased 40-fold in animals administered cinacalcet (**Figure 3.10D**) consistent with the hypothesis that CaSR activation increases renal Cldn14 expression. The renal expression of  $1\alpha$ -OHase was decreased and the expression of 24-OHase was increased significantly (**Table 3.17**).

### 3.4.3 Cldn14 protein expression

An increase in the expression of Cldn14 protein was observed by immunostaining on kidney sections of mice treated with cinacalcet when compared to kidney sections of control mice (**Figure 3.11**).

**Figure 3.10** Cinacalcet experiment: *RNA expression of claudins in whole kidney*

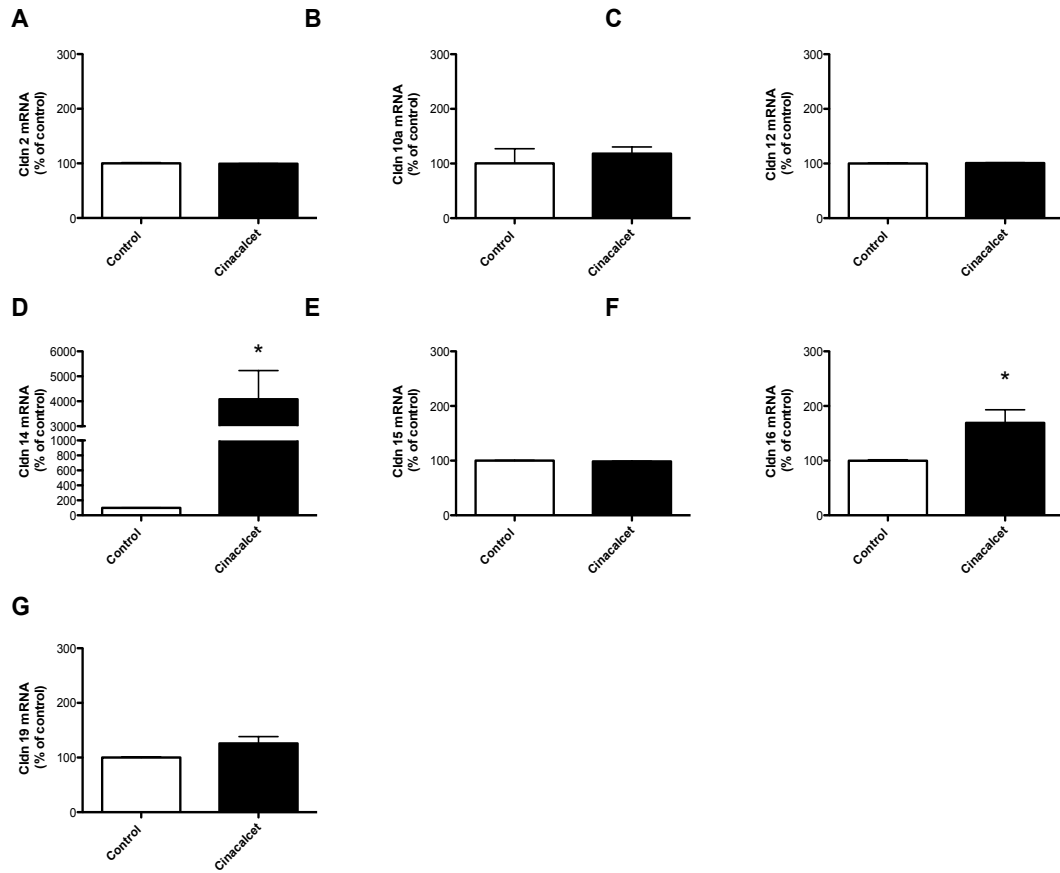


**Figure 3.10:** qPCR analysis of Cldn2 (A), Cldn10a (B), Cldn12 (C), Cldn14 (D), Cldn15 (E), Cldn16 (F), Cldn19 (G) expression in whole kidney of mice on control diet and cinacalcet treated diet. The results are expressed as a percentage of control group and are normalized to the expression of 18S.  $n = 6$  in each group. \* $p < 0.05$  in comparison to control group.

**Table 3.17 Cinacalcet experiment: RNA expression of 1 $\alpha$ -OHase and 24-OHase**

	<b>1<math>\alpha</math>Hydroxylase (%)</b>	<b>24<math>\alpha</math>Hydroxylase (%)</b>
<b>Control</b>	100 $\pm$ 1.26	100 $\pm$ 1.93
<b>Cinacalcet</b>	62.51 $\pm$ 8.08*	353.66 $\pm$ 79.93*

Values are mean  $\pm$  SE.  $n = 6$  in each group. \* $p < 0.05$  when compared with control

**Figure 3.11 Cinacalcet experiment: Immunostaining for Cldn14**

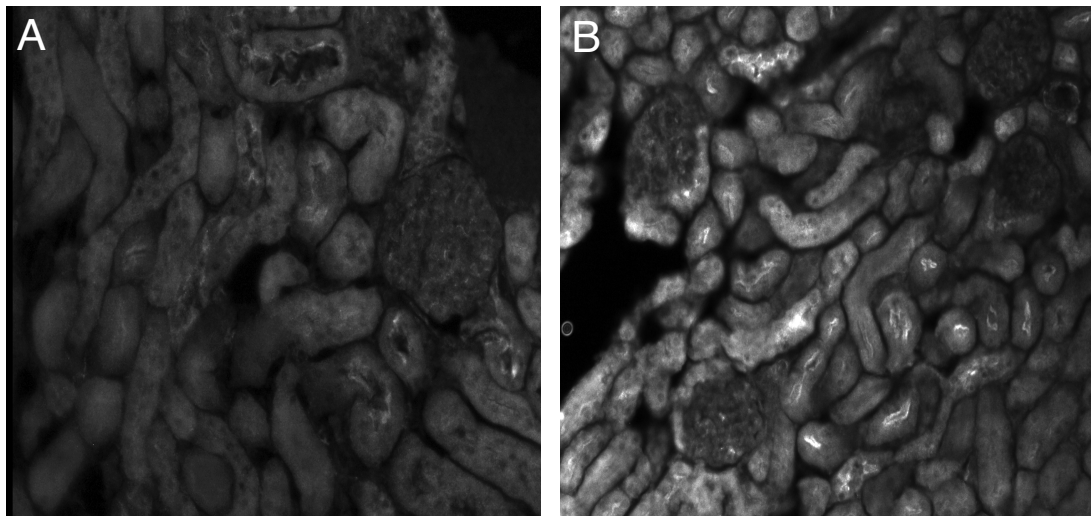


**Figure 3.11:** Low power images of immunostaining for Cldn14 of renal sections of wild type (A) and cinacalcet treated (B) mice.

### **3.5 Localization of Cldn14 in murine kidney**

To study the localization of Cldn14 in murine kidney immunofluorescence dual staining experiments were carried out with various tubular segment markers on kidney sections of mice treated with cinacalcet. Colocalization of Cldn14 was observed with *Lotus Tetragonolobus Lectin*, a proximal tubule marker (**Figure 3.12**). Colocalization was not observed with NKCC2, a TAL marker (**Figure 3.13**).

**Figure 3.12 Immunostaining for Cldn14 in the proximal tubule**

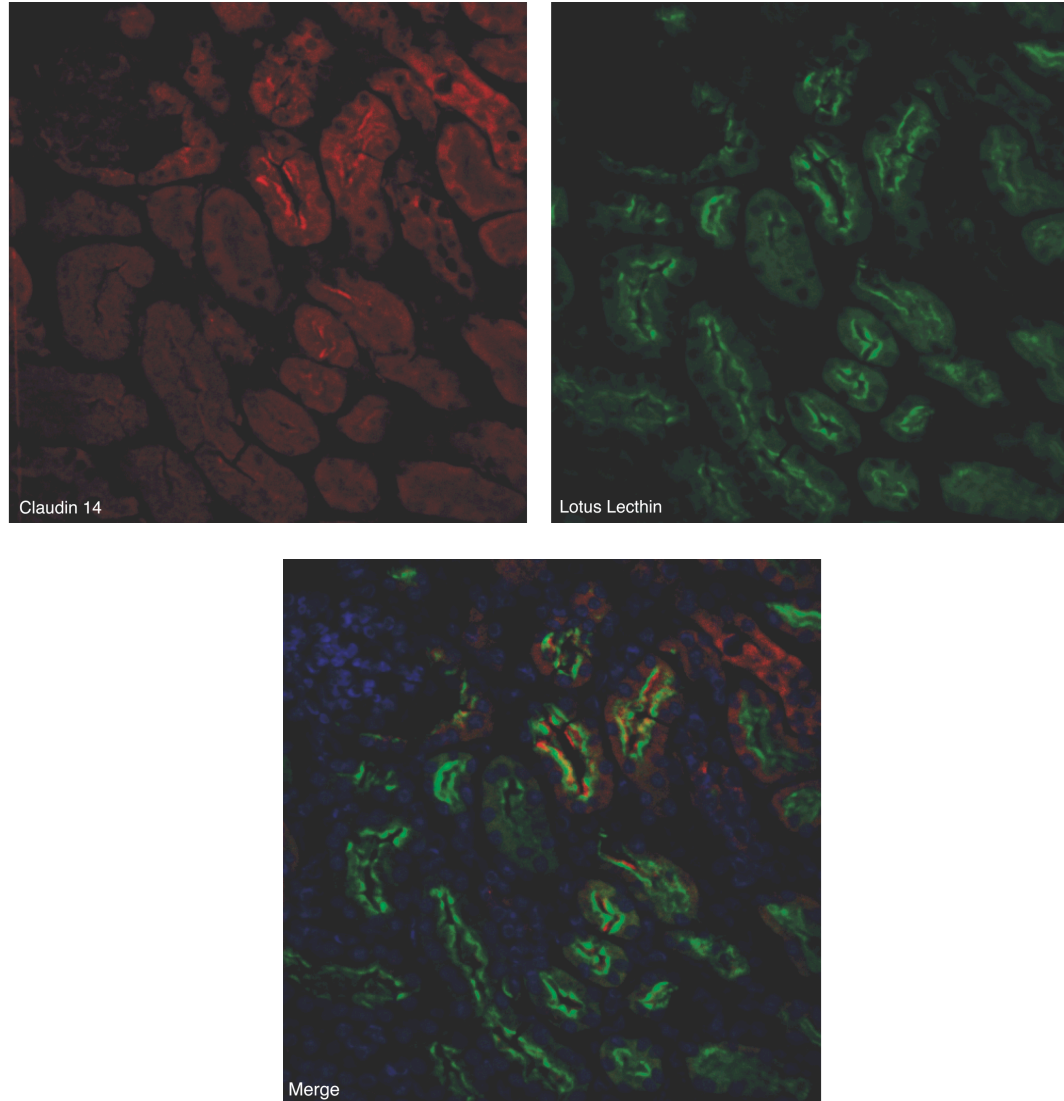


**Figure 3.12:** Low power representative images of kidney sections from mice treated with cinacalcet for the localization of Cldn14 (red) in the proximal tubule; Lotus Lectin (green) was used as a proximal tubule marker; Dapi (blue) is used as a marker for the nucleus.

**Figure 3.13 Immunostaining for Cldn14 in the TAL**

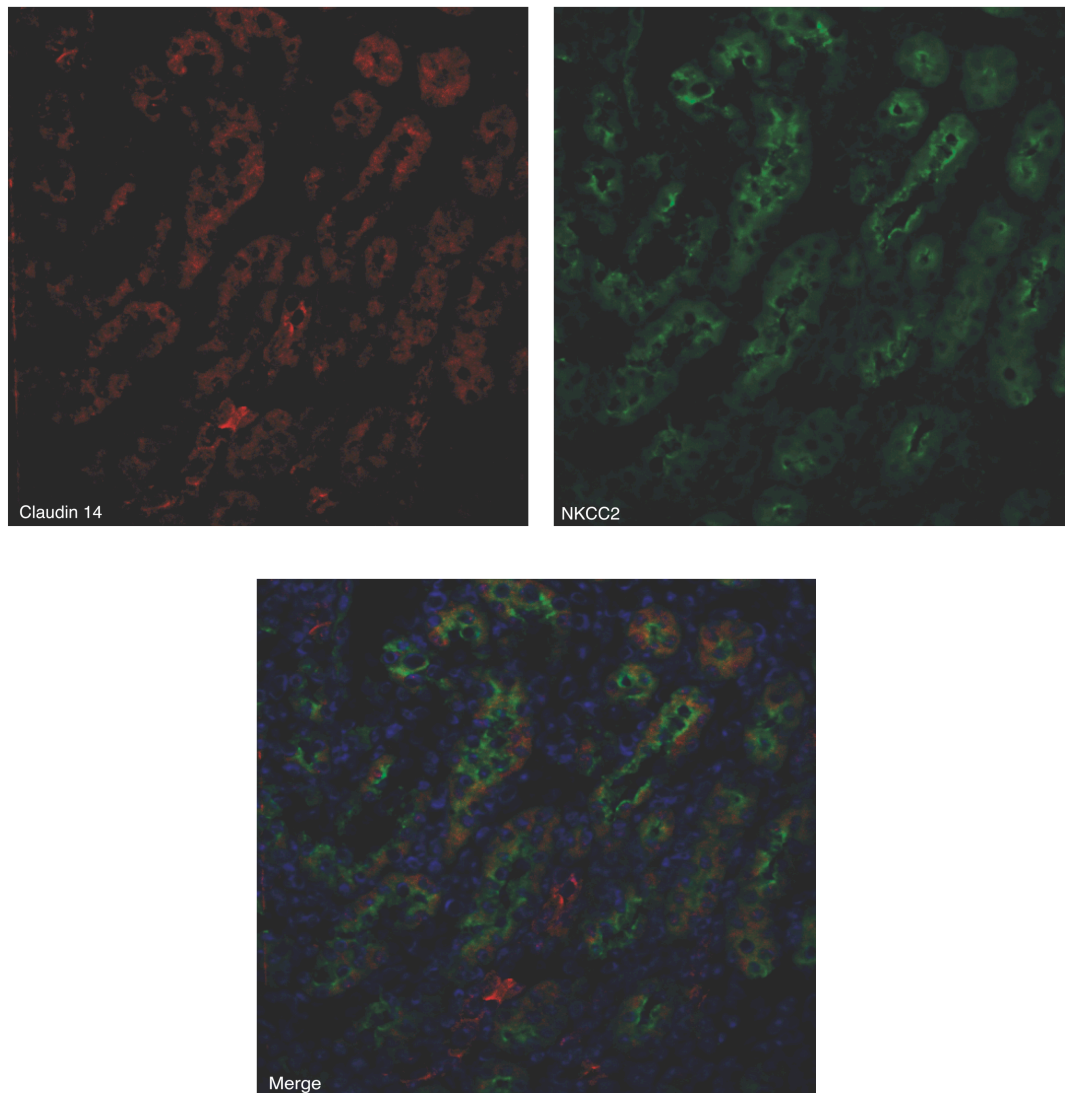


**Figure 3.13:** Low power representative images of kidney sections from mice treated with cinacalcet for the localization of Cldn14 (red) in the TAL; Sodium-potassium-chloride cotransporter (green) is used as a TAL marker; Dapi (blue) is a marker for the nucleus.

**CHAPTER 4**

**DISCUSSION**

The renal regulation of  $\text{Ca}^{2+}$  excretion is central to maintaining serum  $\text{Ca}^{2+}$  concentration within a tight range. When the serum  $\text{Ca}^{2+}$  levels are low it is called hypocalcemia and when the serum  $\text{Ca}^{2+}$  levels are higher than normal it is referred to as hypercalcemia. Alterations in the renal handling of  $\text{Ca}^{2+}$  can cause hypercalciuria, leading to the formation of  $\text{Ca}^{2+}$ -containing kidney stones (Levy, Adams-Huet et al. 1995). The majority of calcium is reabsorbed from the proximal tubule and the TAL by a passive paracellular process. The molecules permitting the passage of ions between cells are claudins. The first part of these studies characterized the expression of claudins in whole kidney and then in the proximal tubule. The CaSR is expressed in the basolateral membrane of the TAL and it plays a central role in regulating renal tubular  $\text{Ca}^{2+}$  reabsorption. However, the downstream mechanisms after CaSR activation have been incompletely elucidated. We provide evidence from these studies that CaSR stimulation prevents paracellular  $\text{Ca}^{2+}$  flux by increasing renal Cldn14 expression. We report that the expression of Cldn14 increases with an increase of free  $\text{Ca}^{2+}$  levels in the serum when mice were subjected to high  $\text{Ca}^{2+}$  diet, administered  $1,25(\text{OH})_2\text{D}_3$  and upon treatment with the calcimimetic cinacalcet. In all three conditions the urinary  $\text{Ca}^{2+}$  /Creatinine ratio increased along with either no change or an increase in ionized  $\text{Ca}^{2+}$  and  $1,25(\text{OH})_2\text{D}_3$ . PTH levels were not detectable when mice were injected with  $1,25(\text{OH})_2\text{D}_3$  or treated with cinacalcet.

#### **4.1 Renal claudin expression**

The renal expression of claudins has not yet been clearly delineated. Except Cldn17 we found all claudins from claudin- 1 to -23 to be present in murine whole kidney. Specifically in the proximal tubule claudin-1, -2, -3, -8, -10a, -10b, -12, -15 and -16 were found to be present. Earlier studies have shown the presence of claudin-2, -6, -9, -10 and -11 in the proximal tubule (Gunzel and Yu, 2009). Cldn6 and Cldn9 are developmentally expressed renal tight junction proteins, which are only expressed in the kidney of neonatal mice (Abuazza, Becker et al. 2006). We did not see the expression of Cldn6 or Cldn9 as we used older mice within the age group of 8-10 weeks. In order to decipher the role of claudins in maintaining ion homeostasis it is of great importance to know the expression pattern of these tight junction proteins and how they vary along the different nephron segments.

#### **4.2 Renal Cldn14 expression**

The expression of Cldn14 in the kidney has been a controversy. Cldn14 has been reported to be expressed in the distal convoluted tubule (Kirk, Campbell et al. 2010) and in the proximal tubule (Ben-Yosef, Belyantseva et al. 2003). This latter finding is at odds with our micro-dissection experiments. However recently, clear evidence of expression of Cldn14 in the thick ascending limb has been provided by Gong et al. (Gong, Renigunta et al. 2012). These authors employed Cldn14 knockout mice where the Cldn14 gene was replaced with beta galactosidase. Immunolocalization studies were carried out on Cldn14<sup>+lacZ</sup> mouse kidneys counterstained for  $\beta$ -galactosidase activity. Their results showed co-localization with Tamm-Horsfall protein, a tubule

marker for TAL. No expression was found in the glomerulus, proximal tubule, distal convoluted tubule or the collecting ducts. This nephron segment expresses the CaSR in its basolateral membrane (Riccardi, Lee et al. 1996; Yang, Hassan et al. 1997), thus permitting the sensing of circulating  $\text{Ca}^{2+}$  levels, consistent with a role for Cldn14 in renal tubular  $\text{Ca}^{2+}$  handling.

A >2-fold increase of renal Cldn 14 expression was observed at the mRNA level in mice on a high  $\text{Ca}^{2+}$  diet. When injected with  $1,25(\text{OH})_2\text{D}_3$  the mRNA level of Cldn14 increased 10-fold and when treated with cinacalcet it increased by 40-fold. The Gong et al study was published while we were attempting to quantify and localize Cldn14 in the renal tubule. We have performed western blotting and immunolocalization studies with 5 different Cldn14 antibodies. The best antibody (Invitrogen, Carlsbad, CA, USA; Catalog # 36-4200) available to us provided strong staining in the renal proximal tubule that was absent in the TAL. Moreover we observed increased expression of Cldn14 in kidneys from vitamin D treated and cinacalcet treated animals. However, the degree of increased staining was not nearly to the same degree as per the change in mRNA expression we observed. This may be because of unknown changes leading to lower expression of Cldn14 protein or due to weak antibody specificity in detecting Cldn14 protein. As we do not have a negative control for these experiments we feel that the proximal tubular staining is likely non-specific and feel that the renal expression of Cldn14 is likely in the TAL as per Gong et al.

### 4.3 Driving forces for calcium flux across the TAL

Paracellular  $\text{Ca}^{2+}$  transport across the TAL depends on a lumen-positive transepithelial voltage and a lumen to blood concentration gradient for  $\text{Ca}^{2+}$ . This gradient appears to be generated by two interdependent mechanisms. The first is the result of asymmetrical secretion of electrolytes, after their influx into TAL epithelial cells. This contributes to a lumen-positive voltage ranging from 5-10 mV (Greger and Schlatter 1983; Greger and Velazquez 1987). The second mechanism is the consequence of  $\text{Na}^+$  backflux into the lumen of the cortical TAL. (Dimke, Hoenderop et al. 2010). This process could potentially further increase transepithelial potential difference to values as high as 30 mV (Rocha and Kokko 1973; Greger 1981; Mandon, Siga et al. 1993; Hou, Paul et al. 2005). In the TAL,  $\text{NaCl}$  reabsorption is a continuous process. This results in the dilution of the tubular fluid that gradually generates a concentration gradient for  $\text{NaCl}$ . It is known that the concentration of  $\text{Na}^+$  in the peritubular space is around 140 mM and goes down to about 30 mM in the lumen. This difference in the concentration generates a lumen positive transepithelial diffusion potential that acts as the driving force for  $\text{Ca}^{2+}$  and  $\text{Mg}^{++}$  from this tubule (Hou, Renigunta et al. 2008). The backflux of  $\text{Na}^+$  across the TAL occurs via a  $\text{Cldn16/Cldn19}$  complex, which forms a cation permeable pore (Hou, Renigunta et al. 2008). This same complex likely also permits the paracellular reabsorption of divalent cations, down their electrochemical gradient. Consequently mutations in  $\text{Cldn16}$  or  $\text{Cldn19}$  reduce cation selectivity of the complex and cause familial hypomagnesemia with hypercalciuria and nephrocalcinosis (FHHNC) (Simon, Lu et al. 1999; Konrad, Schaller et al. 2006; Hou, Renigunta et al. 2008). FHHNC is an autosomal recessive disorder occurring due to

disturbed  $\text{Ca}^{2+}$  and magnesium homeostasis. Occurrence of urinary tract infection, polyuria/polydipsia and calcinosis is very common among patients with FHHNC. Genetic defects include loss of function mutation in the Cldn16 gene (Hampson G, Konrad M et al. 2008) and Cldn19 gene (Naeem M, Hussain S et al. 2011).

#### **4.4 Cldn14, a blocker of the cldn16/19 pore?**

Recently Gong *et. al.* demonstrated that Cldn14 can interact with Cldn16, but not Cldn19 (Gong, Renigunta et al. 2012). However, Cldn16 has the ability to bind both claudins. Therefore, the 3 claudins could potentially exist as a complex. Consistent with this, the coexpression of all 3 claudins significantly reduced  $\text{Na}^+$  permeation relative to overexpression of just Cldn16 and Cldn19 together (Ben-Yosef, Belyantseva et al. 2003; Gong, Renigunta et al. 2012). Data from the Alexander laboratory is in agreement with this observation. Overexpression of Cldn14 in OK cells dramatically reduces  $P_{\text{Na}}$ ,  $P_{\text{Cl}}$ , and the  $P_{\text{Na}}/P_{\text{Cl}}$  ratio, by decreasing  $P_{\text{Na}}$  more than  $P_{\text{Cl}}$  (**Appendix**). Interestingly, we observed a reduction in both  $P_{\text{Na}}$  and  $P_{\text{Cl}}$  in contrast to previous studies. It is likely that the cell model employed is responsible for these subtle differences. Regardless, increased Cldn14 expression in the TAL would prevent  $\text{Ca}^{2+}$  reabsorption by; *i*) reducing the permeability of the pore to  $\text{Ca}^{2+}$  and *ii*) by blocking backflux of  $\text{Na}^+$  and thereby decreasing the electrochemical gradient driving paracellular  $\text{Ca}^{2+}$  flux across this segment.

#### 4.5 Role of Cldn14 in human physiology and pathophysiology

SNP's in the *CLDN14* gene correlate with kidney stone formation, osteopenia and hypercalcaemia. The mechanism through which Cldn14 causes these phenotypes was not clear, since a correlation between the risk variants and mRNA expression of Cldn14 in adipose and peripheral blood samples was not observed (Thorleifsson, Holm et al. 2009). Based on very recent data by Gong *et al.*, (Gong, Renigunta et al. 2012) and this study, it is clear that significant renal Cldn14 expression is strongly dependent on activation of the CaSR. Low baseline renal expression of Cldn14 explains why patients lacking CLDN14 do not demonstrate evidence of altered Ca<sup>2+</sup> homeostasis (*i.e.* stone formation or osteopenia) (Wilcox, Burton et al. 2001), although detailed physiological characterization may demonstrate that they are unable to effectively excrete a Ca<sup>2+</sup> load. Moreover, the urinary excretion of Ca<sup>2+</sup> in Cldn11/Cldn14 double knockout mice was not altered. This provides further evidence that the absence of Cldn14 does not impact the renal handling of Ca<sup>2+</sup> (Elkouby-Naor, Abassi et al. 2008). A critical experiment confirming a role for Cldn14 in renal Ca<sup>2+</sup> handling was recently performed. Cldn14 deficient mice were placed on a high Ca<sup>2+</sup> diet and found to have relative hypomagnesiuria and hypocalciuria in comparison to wild-type controls (Gong, Renigunta et al. 2012). This response would be expected in the absence of the CaSR-Cldn14 axis, as an increased luminal to blood Ca<sup>2+</sup> concentration gradient would favour increased paracellular Ca<sup>2+</sup> reabsorption from the TAL. In addition, this may represent an important mechanism to functionally uncouple Ca<sup>2+</sup> reabsorption from that of NaCl in the TAL.

Autosomal dominant hypocalcaemic hypercalciuria is due to activating mutations in the *CASR* (Pollak, Brown et al. 1994; Pearce, Williamson et al. 1996). Mild asymptomatic hypocalcemia is generally observed in these patients (Pearce, Williamson et al. 1996). These mutations cause the half-maximal activity of the receptor to increase (Pollak, Brown et al. 1994; Pearce, Williamson et al. 1996). More severe activating mutations in the CaSR cause an autosomal dominant form of Bartter's syndrome (Pollak, Brown et al. 1994; Vargas-Poussou, Huang et al. 2002; Watanabe, Fukumoto et al. 2002). These individuals have a classical Bartter-like phenotype, but differ clinically from individuals with classical Bartter's by the presence of suppressed PTH secretion, hypocalcemia, renal Ca<sup>2+</sup> wasting, and nephrocalcinosis. Discovery of the CaSR-Cldn14 axis provides further insight into these symptoms. Activating mutations in the CaSR would increase Cldn14 expression inappropriately, causing renal Ca<sup>2+</sup> wasting and nephrocalcinosis. Polymorphisms in the CaSR have also been implicated in idiopathic hypercalciuria (Vezzoli, Tanini et al. 2002). As both Cldn14 and the CaSR are now part of a common pathway, association studies may increase their power by grouping CaSR and Cldn14 together.

## Summary

Taken together these data infer a mechanism whereby increased circulating  $\text{Ca}^{2+}$  activates the CaSR and causes increased renal Cldn14 expression. This in turn blocks  $\text{Ca}^{2+}$  permeable paracellular pores preventing the increased amount of filtered  $\text{Ca}^{2+}$  from being reabsorped back into the blood. In addition to reducing the transtubular electric gradient, by impairing  $\text{Na}^+$  backflux. Ultimately a  $\text{Ca}^{2+}$  load is excreted, returning circulating  $\text{Ca}^{2+}$  to normal levels (**Figure 4.1**).

**Figure 4.1** Schematic representation of the proposed mechanism of CaSR activation and function of Cldn14 in the TAL

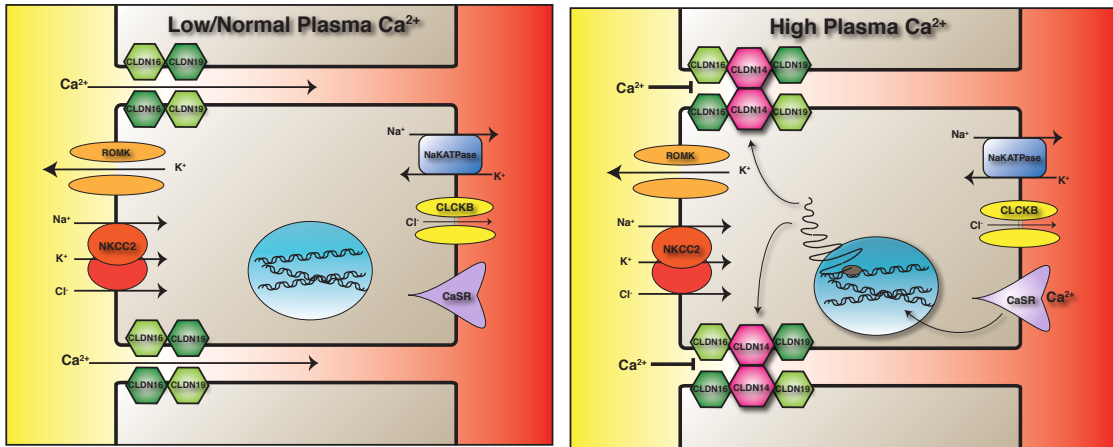


**Figure 4.1:** Schematic representation of the proposed mechanism of CaSR activation and function of claudin-14 in the TAL. During low/normal plasma Ca<sup>2+</sup> levels Ca<sup>2+</sup> flux across the TAL would occur passively via Cldn16 and Cldn19. When plasma Ca<sup>2+</sup> levels are high CaSR on the basolateral membrane gets activated and results in increased expression of Cldn14 at the tight junction ultimately blocking Ca<sup>2+</sup> reabsorption.

## **Conclusion**

Our data identifies all the claudins present in the proximal nephron. Also our experiments indicate that the expression of a specific claudin, Cldn14, is altered by perturbations in calcium homeostasis. Thus, Cldn14 is involved in paracellular calcium flux across the proximal nephron in the kidney.

## **POTENTIAL FUTURE DIRECTIONS**

The importance of CaSR activation and its effects on expression of Cldn14 is yet to be completely established. The next step is to perform *in-situ* hybridization studies to confirm the expression of Cldn14 in the TAL. Primary cell culture studies can then be performed upon the nephron segment expressing Cldn14. *In vitro* studies on an appropriate cell line with different calcimimetics would help delineate the exact molecular mechanism involved in functional activity of Cldn14. Electrophysiological studies on cell culture as well as primary cell culture would help understand the role of Cldn14 in blocking calcium flux across the nephron. Our *in vivo* studies reveal a decrease in PTH under all circumstances where Cldn14 expression is increased (vitamin D administration, high Ca<sup>2+</sup> diet and cinacalcet administration). While unlikely it cannot be excluded that PTH suppresses Cldn14 expression. We have attempted to perform parathyroidectomies on mice to determine the role of isolated PTH suppression, however the presence of ectopic parathyroid glands in this species makes this procedure very difficult if not impossible. When an appropriate cell culture model has been developed it will be important to ascertain the affect of PTH on Cldn14 expression. Ultimately generation of a mouse overexpressing Cldn14 in the TAL would prove the importance of Cldn14 in the maintenance of calcium homeostasis in the body. We predict such an animal should suffer from hypercalciuria.

## **BIBLIOGRAPHY**

- Abuazza, G., A. Becker, et al. "Claudins 6, 9, and 13 are developmentally expressed renal tight junction proteins." Am J Physiol Renal Physiol(2006 Jun 13): 2006 Dec;229(2006):F1132-2041.
- Alexander, R. T., T. E. Woudenberg-Vrenken, et al. (2009). "Klotho prevents renal calcium loss." J Am Soc Nephrol **20**(11): 2371-2379.
- Amasheh, S., N. Meiri, et al. (2002). "Claudin-2 expression induces cation-selective channels in tight junctions of epithelial cells." J Cell Sci **115**(Pt 24): 4969-4976.
- AP, Evan. (2010). "- Physiopathology and etiology of stone formation in the kidney and the urinary." Pediatr Nephrol **25**(5): 831-841.
- Balkovetz, D. F. (2006). "Claudins at the gate: determinants of renal epithelial tight junction paracellular permeability." Am J Physiol Renal Physiol **290**(3): F572-579.
- Ben-Yosef, T., I. A. Belyantseva, et al. (2003). "Claudin 14 knockout mice, a model for autosomal recessive deafness DFNB29, are deaf due to cochlear hair cell degeneration." Hum Mol Genet **12**(16): 2049-2061.
- Bindels R.J., Hartog A. et al (1991). "Active Ca<sup>2+</sup> transport in primary cultures of rabbit kidney CCD: stimulation by 1,25-dihydroxyvitamin D3 and PTH." Am J Physiol **261**(5 pt 2): F 799-807.
- Bushinsky, D. A. and M. J. Favus (1988). "Mechanism of hypercalciuria in genetic hypercalciuric rats. Inherited defect in intestinal calcium transport." The Journal of Clinical Investigation **82**(5): 1585-1591.
- Cole, Z. A., E. M. Dennison, et al. (2008). "Osteoporosis epidemiology update." Curr Rheumatol Rep **10**(2): 92-96.
- Colegio, O. R., C. M. Van Itallie, et al. (2002). "Claudins create charge-selective channels in the paracellular pathway between epithelial cells." American Journal of Physiology - Cell Physiology **283**(1): C142-C147.
- Elkouby-Naor, L., Z. Abassi, et al. (2008). "Double gene deletion reveals lack of cooperation between claudin 11 and claudin 14 tight junction proteins." Cell Tissue Res **333**(3): 427-438.
- Fedric L. (1980). "- Renal handling of calcium and phosphate." Klin Wochenschr **58**(19): 985-1003.
- Fedric L, C., E. Andrew P, et al. (2010). "- Three pathways for human kidney stone formation." Urol Res **38**(3): 147-160.
- Fromter E. and Geßner K. (2001). "Free-Flow Potential Profile along Rat Kidney Proximal Tubule." J Am Soc Nephrol **12**: 2197-2206.

- Fujita, H., H. Chiba, et al. (2006). "Differential expression and subcellular localization of claudin-7, -8, -12, -13, and -15 along the mouse intestine." J Histochem Cytochem **54**(8): 933-944.
- Fujita, H., K. Sugimoto, et al. (2008). "Tight junction proteins claudin-2 and -12 are critical for vitamin D-dependent Ca<sup>2+</sup> absorption between enterocytes." Mol Biol Cell **19**(5): 1912-1921.
- Fujita, H., K. Sugimoto, et al. (2008). "Tight Junction Proteins Claudin-2 and -12 Are Critical for Vitamin D-dependent Ca<sup>2+</sup> Absorption between Enterocytes." Mol Biol Cell **19**(5): 1912-1921.
- García, N. H., C. R. Ramsey, et al. (1998). "Understanding the Role of Paracellular Transport in the Proximal Tubule." Physiology **13**(1): 38-43.
- Garriguet, D. (2011). "Bone health: osteoporosis, calcium and vitamin D." Health Rep **22**(3): 7-14.
- Gong, Y., V. Renigunta, et al. (2012). "Claudin-14 regulates renal Ca<sup>++</sup> transport in response to CaSR signalling via a novel microRNA pathway." Embo J.
- Greger, R. (1981). "Cation selectivity of the isolated perfused cortical thick ascending limb of Henle's loop of rabbit kidney." Pflugers Arch **390**(1): 30-37.
- Greger, R. and E. Schlatter (1983). "Properties of the lumen membrane of the cortical thick ascending limb of Henle's loop of rabbit kidney." Pflugers Arch **396**(4): 315-324.
- Greger, R. and H. Velazquez (1987). "The cortical thick ascending limb and early distal convoluted tubule in the urinary concentrating mechanism." Kidney Int **31**(2): 590-596.
- Gunzel, D., M. Stüiver, et al. (2009). "Claudin-10 exists in six alternatively spliced isoforms that exhibit distinct localization and function." J Cell Sci **122**(Pt 10): 1507-1517.
- Hou, J., D. L. Paul, et al. (2005). "Paracellin-1 and the modulation of ion selectivity of tight junctions." J Cell Sci **118**(Pt 21): 5109-5118.
- Hou, J., A. Renigunta, et al. (2008). "Claudin-16 and claudin-19 interact and form a cation-selective tight junction complex." The Journal of Clinical Investigation **118**(2): 619-628.
- Ikari, A., C. Okude, et al. (2008). "Activation of a polyvalent cation-sensing receptor decreases magnesium transport via claudin-16." Biochimica et Biophysica Acta (BBA) - Biomembranes **1778**(1): 283-290.
- Kawedia, J. D., M. L. Nieman, et al. (2007). "Interaction between transcellular and paracellular water transport pathways through Aquaporin 5 and the tight junction complex." Proceedings of the National Academy of Sciences **104**(9): 3621-3626.

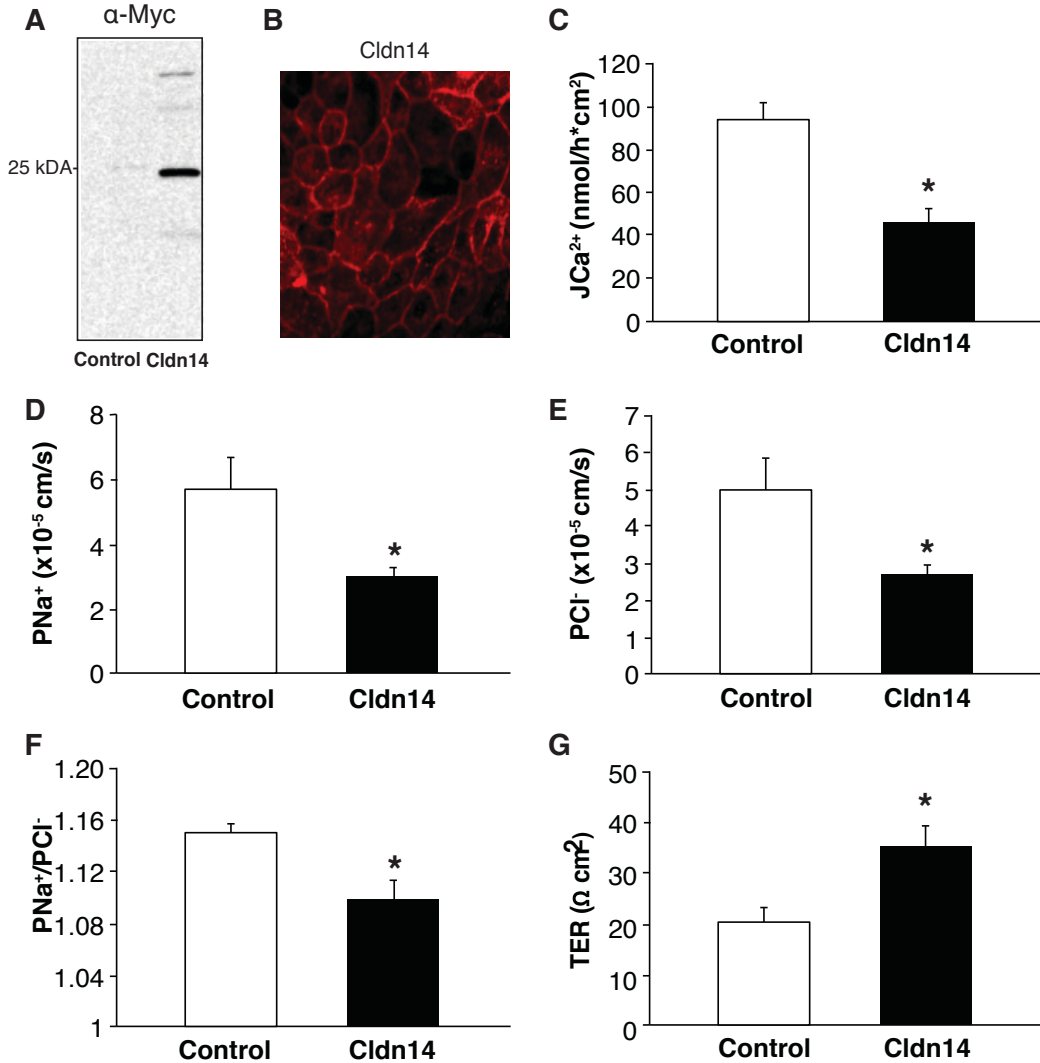
- Khosla, S., L. J. Melton, 3rd, et al. "The unitary model for estrogen deficiency and the pathogenesis of osteoporosis: is a revision needed?" J Bone Miner Res(10): 2011 Mar;2026(2013):2441-2051.
- Kirk, A., S. Campbell, et al. (2010). "Differential expression of claudin tight junction proteins in the human cortical nephron." Nephrol Dial Transplant **25**(7): 2107-2119.
- Kiuchi-Saishin, Y., S. Gotoh, et al. (2002). "Differential expression patterns of claudins, tight junction membrane proteins, in mouse nephron segments." J Am Soc Nephrol **13**(4): 875-886.
- Komm, B. S. and S. Mirkin (2012). "Incorporating bazedoxifene/conjugated estrogens into the current paradigm of menopausal therapy." Int J Womens Health **4**: 129-140.
- Konrad, M., A. Schaller, et al. (2006). "Mutations in the tight-junction gene claudin 19 (CLDN19) are associated with renal magnesium wasting, renal failure, and severe ocular involvement." Am J Hum Genet **79**(5): 949-957.
- Kokko P. (1973). "Proximal Tubule Potential Difference dependence on glucose, HCO<sub>3</sub> and amino acids." J Clin Invest **52**: 1362-1367.
- Lambers, T. T., R. J. Bindels, et al. (2006). "Coordinated control of renal Ca<sup>2+</sup> handling." Kidney Int **69**(4): 650-654.
- Levy, F. L., B. Adams-Huet, et al. (1995). "Ambulatory evaluation of nephrolithiasis: an update of a 1980 protocol." Am J Med **98**(1): 50-59.
- Li, J., W. Ananthapanyasut, et al. (2011). "Claudins in renal physiology and disease." Pediatr Nephrol **26**(12): 2133-2142.
- Luyckx, V. A., B. Leclercq, et al. (1999). "Diet-dependent hypercalciuria in transgenic mice with reduced CLC5 chloride channel expression." Proceedings of the National Academy of Sciences **96**(21): 12174-12179.
- Milica, B. and Valdivielso. JM (2012). "- Calcium signaling in renal tubular cells." Adv Exp Med Biol **740**: 933-944.
- Mandon, B., E. Siga, et al. (1993). "Ca<sup>2+</sup>, Mg<sup>2+</sup> and K<sup>+</sup> transport in the cortical and medullary thick ascending limb of the rat nephron: influence of transepithelial voltage." Pflugers Arch **424**(5-6): 558-560.
- Matsunuma, A. and N. Horiuchi (2007). "Leptin attenuates gene expression for renal 25-hydroxyvitamin D3-1alpha-hydroxylase in mice via the long form of the leptin receptor." Arch Biochem Biophys **463**(1): 118-127.
- Murer, H., G. Ahearn, et al. (1983). "Co- and counter-transport mechanisms in brush border membranes and basal-lateral membranes of intestine and kidney." Journal of Experimental Biology **106**(1): 163-180.

- Muto, S., M. Hata, et al. (2010). "Claudin-2-deficient mice are defective in the leaky and cation-selective paracellular permeability properties of renal proximal tubules." Proceedings of the National Academy of Sciences **107**(17): 8011-8016.
- Nowson C.A., McGrath J.J., et al. (2012). "Vitamin D and health in adults in Australia and New Zealand: a position statement." Med J Aust **196**(11): 686-687.
- Otomo-Corgel, J. (2000). "Osteoporosis and osteopenia: implications for periodontal and implant therapy." Periodontol **59**(1): 111-139.
- Pak, C. Y., K. Sakhaee, et al. (2011). "Defining hypercalciuria in nephrolithiasis." Kidney Int **80**(7): 777-782.
- Papapoulos S.E. (2008). "Bisphosphonates: how do they work?." Best Practicw & Research Clinical Endocrinology & Metabolism **22**(5): 831-847.
- Pearce, S. H., C. Williamson, et al. (1996). "A familial syndrome of hypocalcemia with hypercalciuria due to mutations in the calcium-sensing receptor." N Engl J Med **335**(15): 1115-1122.
- Pollak, M. R., E. M. Brown, et al. (1994). "Autosomal dominant hypocalcaemia caused by a Ca(2+)-sensing receptor gene mutation." Nat Genet **8**(3): 303-307.
- Rathi, S., W. Kern, et al. (2007). "Vitamin C-induced hyperoxaluria causing reversible tubulointerstitial nephritis and chronic renal failure: a case report." Journal of Medical Case Reports **1**(1): 155.
- Riccardi, D., W. S. Lee, et al. (1996). "Localization of the extracellular Ca(2+)-sensing receptor and PTH/PTHrP receptor in rat kidney." Am J Physiol **271**(4 Pt 2): F951-956.
- Razzaque M.S. (2011). "The dualistic role of vitamin D in vascular calcification." Kidney Int. **79**(7): 708--714
- Rocha, A. S. and J. P. Kokko (1973). "Sodium chloride and water transport in the medullary thick ascending limb of Henle. Evidence for active chloride transport." J Clin Invest **52**(3): 612-623.
- Rule, A. D., V. L. Roger, et al. (2010). "Kidney Stones Associate with Increased Risk for Myocardial Infarction." Journal of the American Society of Nephrology **21**(10): 1641-1644.
- Samelson, E. J. and M. T. Hannan (2006). "Epidemiology of osteoporosis." Curr Rheumatol Rep **8**(1): 76-83.
- Schissel, B. L. and B. K. Johnson (2011). "Renal stones: evolving epidemiology and management." Pediatr Emerg Care **27**(7): 676-681.
- Simon, D. B., Y. Lu, et al. (1999). "Paracellin-1, a renal tight junction protein required for paracellular Mg<sup>2+</sup> resorption." Science **285**(5424): 103-106.

- Suki, W. N. (1979). "Calcium transport in the nephron." American Journal of Physiology - Renal Physiology **237**(1): F1-F6.
- Suzuki, Y., C. P. Landowski, et al. (2008). "Mechanisms and Regulation of Epithelial Ca<sup>2+</sup> Absorption in Health and Disease." Annual Review of Physiology **70**(1): 257-271.
- Tamura, A., H. Hayashi, et al. (2011). "Loss of claudin-15, but not claudin-2, causes Na<sup>+</sup> deficiency and glucose malabsorption in mouse small intestine." Gastroenterology **140**(3): 913-923.
- Tarride, J.-E., N. Guo, et al. (2012). "The burden of illness of osteoporosis in Canadian men." Journal of Bone and Mineral Research:
- Thorleifsson, G., H. Holm, et al. (2009). "Sequence variants in the CLDN14 gene associate with kidney stones and bone mineral density." Nat Genet **41**(8): 926-930.
- Torres, P. U., D. Prie, et al. (2007). "Klotho: an antiaging protein involved in mineral and vitamin D metabolism." Kidney Int **71**(8): 730-737.
- Van Itallie CM, Holmes J, et al. (2008). "The density of small tight junction pore varies among cell types and is increased by expression of claudin-2." J Cell Sci **121**:298-305
- Vargas-Poussou, R., C. Huang, et al. (2002). "Functional characterization of a calcium-sensing receptor mutation in severe autosomal dominant hypocalcemia with a Bartter-like syndrome." J Am Soc Nephrol **13**(9): 2259-2266.
- Vezzoli, G., A. Tanini, et al. (2002). "Influence of calcium-sensing receptor gene on urinary calcium excretion in stone-forming patients." J Am Soc Nephrol **13**(10): 2517-2523.
- Watanabe, S., S. Fukumoto, et al. (2002). "Association between activating mutations of calcium-sensing receptor and Bartter's syndrome." Lancet **360**(9334): 692-694.
- Wilcox, E. R., Q. L. Burton, et al. (2001). "Mutations in the gene encoding tight junction claudin-14 cause autosomal recessive deafness DFNB29." Cell **104**(1): 165-172.
- Worcester, E. M. and F. L. Coe (2008). "Nephrolithiasis." Prim Care **35**(2): 369-391, vii.
- Worcester, E. M. and F. L. Coe (2008). "New insights into the pathogenesis of idiopathic hypercalciuria." Semin Nephrol **28**(2): 120-132.
- Yang, T., S. Hassan, et al. (1997). "Expression of PTHrP, PTH/PTHrP receptor, and Ca<sup>2+</sup>-sensing receptor mRNAs along the rat nephron." Am J Physiol **272**(6 Pt 2): F751-758.
- Yu AS, Cheng MH, Angelow S, et al. (2009). "Molecular basis for cation selectivity in claudin-2-based paracellular pores: identification of an electrostatic interaction site." J Gen Physiol **133**:111-127.

## APPENDIX

### OK cells experiment: Overexpression of Cldn14, $\text{Ca}^{2+}$ flux, Ussing's chamber studies



Overexpression of Cldn14 with a *myc* tag in OK cells. Immunoblot blotted for *myc* showing a band at 25 kDa (A), immunostaining of *myc* (B),  $\text{Ca}^{2+}$  flux studies across a monolayer of Cldn14-*myc* overexpressing cells (C),  $\text{PNa}^+$ ,  $\text{PCl}^-$ , and the  $\text{PNa}^+/\text{PCl}^-$  ratio using Ussing's chamber (D-F) and the transepithelial resistance (TER) (G) across OK cells overexpressing Cldn14. \* $p \leq 0.05$  when compared with control. (These experiments were carried out by Wanling Pan and Jelena Borovac).